Author

Susan E. Alford

Title

MICROBIAL SULFATE REDUCTION DURING LOW-TEMPERATURE ALTERATION OF THE LOWER OCEANIC CRUST: INSIGHTS FROM ODP HOLE 735B

submitted in partial fulfillment
of the requirements for the degree of
Master of Science in Oceanography
Department of Geological Sciences
The University of Michigan

Accepted by:

_____	Jeffrey C. Alt	7/30/09
Signature	Name	Date
_____	Stephen E. Kesler	8/6/09
Signature	Name	Date
_____	Samuel B. Mukasa	8/6/09
Department Chair	Name	Date
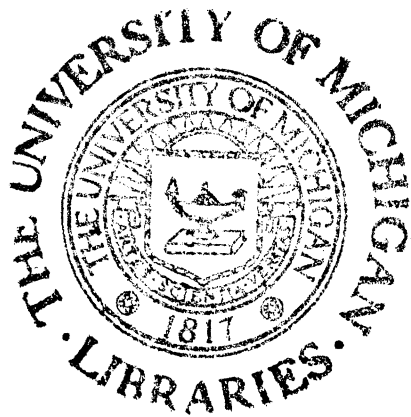
To Harold Dorr

For teaching me to keep my shoes on, even when jumping in head-first.

ACKNOWLEDGEMENTS

TABLE OF CONTENTS

LIST OF FIGURES

FIGURE

LIST OF TABLES

TABLE

ABSTRACT

MICROBIAL SULFATE REDUCTION DURING LOW-TEMPERATURE ALTERATION OF THE LOWER OCEANIC CRUST: INSIGHTS FROM ODP HOLE 735B

by

Susan E. Alford

Sulfide mineralogy was studied in conjunction with measurements of sulfur contents and sulfur isotopes in gabbros from ODP Hole 735B to constrain the mechanisms involved in sulfur cycling during low-temperature seawater alteration of the lower oceanic crust. Most samples have low $SO_4/\Sigma S$ values (≤ 0.15), have retained primary sulfide globules of pyrrhotite $\pm$ chalcopyrite $\pm$ pentlandite and commonly host secondary sulfides as aggregations of pyrrhotite and pyrite laths in assemblages of smectite $\pm$ iron-oxyhydroxide $\pm$ magnetite $\pm$ calcite replacing olivine and clinopyroxene. In comparison to fresh gabbro containing ~ 600 ppm sulfur and $\delta^{34}S$ of 0.1‰, our data indicate an overall addition of sulfide sulfur during low-temperature alteration that varies with depth, accompanied by an overall enrichment in ^{34}S resulting in an average $\delta^{34}S_{Total}$ of 6.4‰. Selection of samples based on the presence of vein minerals formed at temperatures $\leq 110^{\circ}C$ constrains microbial sulfate reduction as the only viable mechanism for the observed sulfide addition, which may have been enabled by the production of H_2 from oxidation of associated olivine and pyroxene. Within these reduced samples, a range in $\delta^{34}S_{sulfide}$ values from -1.5 to 16.3‰ and additions of greater than 900 ppm sulfide among associated sub-samples indicate that reduction of sulfate proceeded under a combination of open and closed system pathways. The few samples that have high $SO_4/\Sigma S$ (≥ 0.46) generally lack secondary sulfides and primarily host trace porous igneous sulfides $\pm$ globular chalcocite and pentlandite within vermicular smectite. These samples contain low concentrations of sulfur (<200 ppm) and range in $\delta^{34}S_{sulfide}$ from 0.7 to 16.9‰, implying the involvement of microbial oxidation of igneous sulfides to produce the elevated $\delta^{34}S_{sulfide}$ values. A late stage of oxidized seawater penetrated locally into the lower 1000 m of Hole 735B and allowed for oxidation of secondary pyrrhotite to secondary laths of pyrite while preventing further additions of sulfur to the gabbro. Our results show that under appropriate temperature conditions, a subsurface biosphere can persist in the lower oceanic crust and alter its geochemistry.

INTRODUCTION

Submarine hydrothermal circulation enables the exchange of chemical components between the seawater, crustal and biological reservoirs. Chemical reactions at submarine hydrothermal sites buffer magnesium and sulfate concentrations of seawater (Edmond et al., 1979b), alter the geochemistry of the lithosphere introduced to subduction zones (Edmond et al., 1979b; Zindler and Hart, 1986) and lead to the formation of massive sulfide deposits (Edmond et al., 1979b; Robb, 2004). Additionally, fluid-rock interaction at and below the seafloor supports chemosynthetically based biological communities that can impose further chemical changes to the seawater and crustal reservoirs (Edwards et al., 2005).

Overview of Submarine Hydrothermal Circulation

Ambient bottom seawater is introduced into the oceanic lithosphere through permeable zones of connected pore-spaces and fractures in the brittle upper oceanic crust (Fisher, 1998). Along the axis of seafloor spreading centers heat provided by magmatic bodies at depth progressively heats the infiltrating seawater, resulting in precipitation of anhydrite as subsurface temperatures reach $150^{\circ}C$, and later production of hydrothermal fluids within deep "reaction zones" as seawater is reacted with middle crustal rocks at temperatures in excess of $350^{\circ}C$ (Alt, 1995a). The high-temperature interactions within the deep reaction zone leach igneous sulfides from the rock to mobilize sulfur as hydrogen sulfide (H_2S), and cause the H_2S-rich hydrothermal fluids to become buoyant and rise through the subsurface (Alt, 1995a; Lister, 1982). Upon ascent, the hydrothermal fluids may cool and mix with seawater to form anhydrite and sulfide precipitates in the shallow volcanic section, or be vented into bottom seawaters by focused discharge of the hydrothermal fluids along axis (Alt 1995; Edmond et al., 1979a; Edmond et al., 1979b).

The crust emplaced at mid-ocean ridges is gradually distanced from the high-temperature magmatic heat source at the ridge by tectonic extension, thereby resulting in a continual reconfiguration of the hydrothermal system governed by fracturing, dissolution and mineralization as the system transforms from an "active" circulation system driven by an underlying heat source at the ridge axis, to a "passive" circulation system driven by residual heat within cooling oceanic lithosphere along the ridge-flanks at temperatures below $150^{\circ}C$ (Alt, 1995a; Alt, 2004; Jacobson, 1992; Lister, 1982). The interaction between low-temperature, oxygenated seawater and the upper ocean crust in these environments leads to the loss of sulfide minerals by oxidation to dissolved sulfate, and loss of anhydrite by dissolution due to its retrograde solubility (Alt, 2004). Furthermore, in contrast to the higher-temperature axial environments, inorganic sulfate reduction cannot actively fix sulfur into the crust in the low-temperature ridge-flank environments because abiotic reduction of dissolved sulfate is inhibited by slow reaction kinetics at temperatures below $150^{\circ}C$ (Goldstein and Aizenshtat, 1994; Malinin and Khitarov, 1969; Ohmoto and Golhaber, 1997;

Ohmoto and Lasaga, 1982). However, textural evidence in conjunction with the presence of DNA and nucleic acids in altered submarine glasses (Fisk et al., 1998; Furnes and Staudigel, 1999; Torsvik et al., 1998) and sampling of ridge-flank fluids (Cowen et al., 2003; Huber et al., 2006) indicate an active presence of microorganisms in subsurface ridge-flank environments. In particular, sulfur isotope data (Alt et al., 2003; Rouxel et al., 2008) provides evidence for the addition of sulfur to the upper oceanic crust under low-temperature, reducing conditions by microbial sulfate reduction. Based on modeling of seawater entrainment and fluid flow within ridge flanks, such biologically-mediated reactions within the upper oceanic crustal environments of ridge-flanks may persist for up to 20 My (Hutnak et al., 2008).

Alteration in Slow-Spreading Systems

Numerous exposures of the lower oceanic crust and upper mantle are present along the sealfoor. These "oceanic core complexes" are inherent to the structure of slower spreading ridges and result from the exhumation of overlying material and subsequent uplift of lower basement sections along detachment faults in response to relatively low magma budgets and asymmetric extension (Carbotte and Sheirer, 2004; Karson, 1998). During uplift and cooling of the basement block, formation of brittle fractures provide for the penetration of seawater and consequent late-stage alteration of the uplifted material (Karson, 1998).

Drilling of an exposed gabbroic oceanic core complex at ODP Site 735 to a depth of 1.5 km allowed for the first significant recovery of an in-situ section of lower oceanic crust (Shipboard Scientific Party, 1999). Initial studies of recovered material indicate relatively low temperatures of $\leq 250^{\circ}C$ during late-stage alteration of the lower 1000 m of the core accompanied by local additions of sulfur (Shipboard Scientific Party, 1999 and Bach et al., 2001). Here, we present the results of a sulfur isotope investigation of the lower 1 km of Hole 735B to explore the evidence for microbial sulfate reduction as a mechanism for the addition of sulfur to the lower oceanic crust. Our results also provide evidence for microbial sulfide oxidation of sulfide minerals within localized sections of the core.

GEOLOGICAL SETTING OF SITE 735

ODP Site 735 is located on Atlantis Bank, an exposure of lower oceanic crustal material near the top of a transverse ridge along the Atlantis II Fracture Zone at 32°43.392'S, 57°15.960'E [Figure 1]. This portion of crust has been dated at 11.5 my and is inferred to have been formed at the ultra-slow spreading Southwest Indian Ridge (SWIR) and later exposed by detachment faulting at 11 mya as an oceanic core complex at the intersection of the paleo-SWIR and the Atlantis II Fracture Zone. Hole 735B was drilled at this site to a depth of ~500 meters below seafloor (mbsf) on ODP Leg 118, and later extended to a final depth of 1508.0 mbsf during ODP

2

Leg 176. Recovery of drilled material from Hole 735B was extremely high for both Legs 118 and 176, averaging ~87% (Shipboard Scientific Party, 1999).
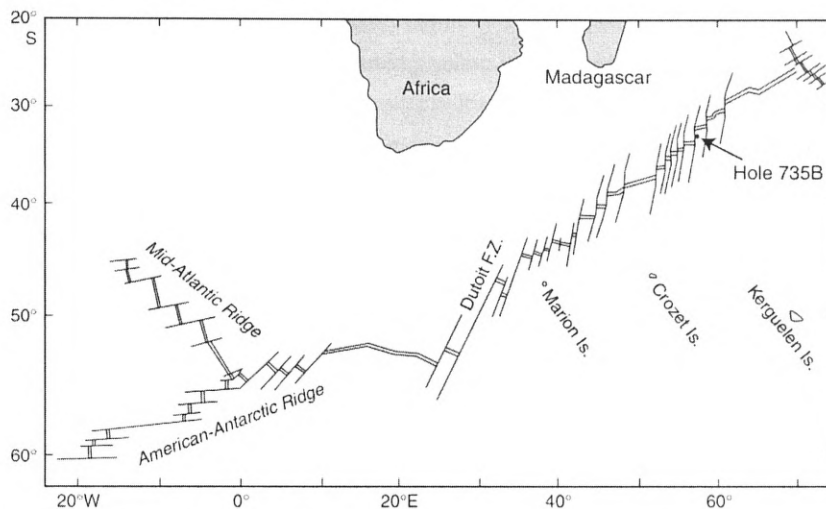
Figure 1. Location map for ODP Hole 735B. (Natland et al., 2002)

The material recovered from Hole 735B has been divided into 12 separate lithologic units that have been defined based on grain size and primary modal mineralogy [Table 1]. The applied classification scheme follows the International Union of Geological Sciences system with some modifications such that "disseminated oxide gabbros" contain 1 to 2% Fe-Ti oxides, "oxide gabbros" contain greater than 2% Fe-Ti oxides, "gabbronorites" contain > 5% orthopyroxene and the modifier "troctolitic" defines gabbros with 5 to15% clinopyroxene. (Shipboard Scientific Party, 1999).

Table 1. Lithologic units of Hole 735B

Drill Leg	Unit	Base of Unit		Lithology
		Leg-section-interval, cm	Depth* (mbsf)	
	I	735B-118-10D-1, 70	37.41	Gabbronorite
LEG 118	II	-35R-6, 72	170.22	Upper Compound Olivine Gabbro
	III	-46R-2, 150	223.57	Disseminated Oxide-Olivine Gabbro
	IV	-56R-3, 116	274.06	Massive Oxide Olivine Gabbro
	V	-74R-6, 3	382.40	Massive Olivine Gabbro
-----	VI	-176-93R-5, 33	537.37	Lower Compound Olivine Gabbro
	VII	-103R-3, 78	600.76	Gabbronorite & Oxide Gabbronorite
	VIII	-115R-6, 81	669.84	Olivine Gabbro
LEG 176	IX	-120R-3, 142	714.35	Gabbronorite & Gabbro
	X	-149 R-1, 73	961.23	Olivine Gabbro & Gabbro
	XI	-188R-6, 14	1314.12	Olivine Gabbro
	XII	-93R-5, 33	1508.00	Olivine Gabbro & Troctolitic Gabbro

*Basal depth of lithologic units as presented by Dick et al., (1991) and Shipboard Scientific Party (1999).

A series of events led to variations in the type and distribution of alteration effects with depth in Hole 735B. Initial dynamothermal metamorphism during exhumation of overlying crustal material resulted in crystal-plastic deformation concentrated as zones of highly-foliated rock, predominately in the upper 200 m. Subsequent cooling and cracking allowed for the formation of brittle fractures and sub-vertical amphibole veins in the upper 700 m, and mediated high-temperature "static alteration" manifested as coronas of amphibole ± talc surrounding pyroxene and olivine. Later cooling and uplift of the ridge led to further fracturing and penetration of cold seawater, forming late-stage smectite, chlorite, carbonate, and zeolite ± prehnite veins throughout Hole 735B. (Shipboard Scientific Party, 1999)

Initial studies indicated a general loss of sulfur to hydrothermal fluids due to the breakdown of igneous sulfides during high-temperature (>350°C) dynamothermal metamorphism, and local oxidation by late-stage circulation of seawater throughout the upper 500 m section recovered during Leg 118 (Alt and Anderson, 1991). Abundant sulfide minerals and high sulfur contents formed in a massive oxide olivine gabbro unit (Lithologic unit IV) within this upper 500 m, as the result of igneous fractionation and concentration of sulfides and oxides (Alt and Anderson, 1991). Further study following recovery of the lower 1 km during Leg 176 led to definition of eight low-temperature alteration zones for the material recovered from Hole 735B based on geochemical differences between relatively fresh and more extensively altered samples [Table 2] (Bach et al., 2001). Bach et al. (2001) illustrated that in correlation with the defined low-temperature alteration zones, sulfur has been both added and lost during low-temperature alteration of 735B.

Table 2. Low-temperature alteration zones of Hole 735B.

Alteration Zone	Depth Range (mbsf)	Alteration Type	Chemical Changes
1'	0-40	Oxidative	+ ^{16}O
2'	40-500	Nonoxidative	+ ^{16}O
1	500-600	Oxidative	+ ^{18}O, C
2	600-835	Nonoxidative	+ C, ^{18}O, S
3	835-1050	Nonoxidative	---
4	1050-1300	Nonoxidative	+ C, ^{18}O, S
5	1300-1475	Nonoxidative	+ C, ^{18}O
6	1475-1508	Greenschist facies	+ ^{16}O

Adapted from (Bach et al., 2001).

METHODS

Sample Selection

Fifteen whole-rock samples from low-temperature alteration zones 1 through 5 and three paired whole-rock sub-samples from low-temperature alteration zone 2 were selected for study based on the presence of iron-oxyhydroxide, calcite, smectite and zeolite in reference to published $\delta^{18}O$ analyses from 735B (Alt and Bach, 2001) which indicate formation temperatures of $\leq 110^oC$ for these minerals. The paired sub-samples are characterized by associated low-temperature alteration halos, which allowed for separation into associated "minimally altered" and "highly altered" sub-samples. The upper limit of 110^oC was applied during sample selection to identify samples formed within the temperature limits of microbial sulfate reducers (Jørgensen, 1992; Seal, 2006) and below the lower temperature limits at which inorganic and thermochemical sulfate reduction become viable mechanisms for sulfide production in seafloor hydrothermal systems (Ohmoto and Lasaga, 1982). For samples that also hosted higher temperature alteration phases such as chlorite or actinolite veins (176-735B-150R-3, 56-62 cm and 176-735B-177R-5, 61-66 cm), the portion containing the higher temperature alteration phase was cut and removed from the sample prior to processing. For this study, no samples were chosen from alteration zone 6 (1475-1506 mbsf), as this zone is characterized by greenschist-facies assemblages (Bach et al., 2001) and whole-rock $\delta^{18}O$ values that are depleted relative to primary gabbroic material (Alt and Bach, 2006), thereby indicating alteration temperatures in excess of 250^oC in this zone.

Petrography & Microprobe Analysis

Each of the samples selected for analysis was examined in hand specimen and thin section under transmitted and reflected light to document petrogenic relationships. Following these characterizations, eight samples representing alteration effects typical of different lithologic unit and alteration zone combinations were selected for compositional analysis of sulfides on a CAMECA SX-100 Electron Microprobe Analyzer. Operating conditions were the following: 20 kV accelerating voltage; 20 nA sample current; 1 μm spot size. Identification of sulfides was based on diagnostic properties of various sulfides in reflected light (Craig and Vaughan, 1981), and was then verified by comparison of electron microprobe analyses with published mineral data (Anthony et al., 1990) and by comparison of calculated formulas to the ideal stoichiometric formula of the relevant sulfide.

Sample Preparation and Sulfur Extractions

In preparation for sulfur extractions, sample surfaces were abraded with an aluminum oxide tipped dremel tool and air-blasted to remove any surface contamination that may have been introduced during coring or later sawing and handling of the rock material. Samples were

then broken in a steel jaw crusher, and powdered in a tungsten carbide shatterbox to homogenize individual samples and to allow for complete reaction of samples during digestions as it has been shown that the reactivity of sulfides using the prescribed extraction methods is dependent on grain size (Backlund et al., 2005; Canfield et al., 1986; Rice et al., 1993). To avoid contamination, all equipment was scrubbed with water, rinsed with 70% ethyl alcohol, and air-blasted between processing of each sample.

After powdering, samples were dried overnight at $100^{o}C$ and stored in a dessicator under vacuum until digestion. As sulfur in MORB often occurs in the form of various sulfide minerals as well as sulfates, each characterized by different $\delta^{34}S$ (Sakai et al., 1984), three separate fractions of sulfur were extracted from ~ 9.5g (weighed to a precision of 0.1 mg) of individual sample powders following a digestion sequence producing H_2S from targeted sulfur forms. Following the procedures of Rice et al (1983) and Tuttle et al. (1986), an acid-volatile sulfide (AVS) fraction was extracted by reaction of sample powders in 6N HCl with $SnCl_2$ for five minutes under boiling conditions, followed by reaction under sub-boiling conditions for 30 minutes. After recovery of the AVS fraction, a chromium-reduced sulfide (CRS) fraction representative of mainly disulfides was extracted by using an acidified $CrCl_2$ solution (Canfield et al., 1986; Zhabina and Volkov, 1978) where contents of the reaction vessel were boiled for 1-2 hours. The final digestion in the extraction procedure targeted sulfates by boiling the remaining contents in the reaction vessel for 2-3 hours with a solution of $HCl + H_3PO_2 + HI$ modified from Thode (1961). All digestions were carried out sequentially within a closed reaction vessel through which N_2 gas continuously flowed to serve as a carrier gas to transport evolved H_2S to a precipitation trap and to establish a reduced atmosphere within the extraction system during digestions. Following extractions, the weight of the recovered Ag_2S precipitates was determined gravimetrically for each fraction. Ag_2S fractions were then transferred to clean vials for storage until isotope analysis. For additional reference, a detailed description of the sulfur extraction procedure addressing relevant analytical considerations is presented in Appendix 1.

Sulfur Isotope Analysis

The Ag_2S precipitates from the recovered sulfur fractions were analyzed for sulfur isotope composition at the United States Geological Survey stable isotope laboratory in Denver, Colorado. The precipitates were combusted to SO_2 with an elemental analyzer and introduced directly via continuous flow mode to a Micromass Optima mass spectrometer for measurement of $^{34}S/^{32}S$ ratios. Results are reported in δ-notation relative to Vienna Canyon Diablo Troilite (V-CDT) in parts per thousand (‰) according to equation 1:

$$\delta^{34}S_{sample} = \frac{(^{34}S/^{32}S)_{sample} - (^{34}S/^{32}S)_{standard}}{(^{34}S/^{32}S)_{standard}} \times 1000 \qquad (1)$$

where the $\delta^{34}S$ of the synthetically produced silver sulfide standards IAEA-S-1 and IAEA-S-2 have been defined as -0.3‰ and 22.67‰ relative to V-CDT and the original CDT sulfur standard (Coplen and Krouse, 1998). Replicate measurements of standards were reproducible to ± 0.2‰. Due to limits of detection, only Ag_2S precipitates that weighed at least 1mg were analyzed. Use of the recently defined V-CDT scale is necessary due to depletion of the original CDT standard, and also allows for greater precision than what has been achievable using the naturally occurring heterogeneous CDT (Beaudoin et al., 1994).

RESULTS

Petrography

Results of representative microprobe analyses of sulfide minerals are presented in Appendix 2. Two different types of sulfide minerals were analyzed, termed as "igneous sulfides" and "secondary sulfides" based on mode of occurrence. Igneous sulfides are defined here as large sulfide globules within igneous silicate grains or interstitial areas and may or may not be rimmed by alteration minerals. Secondary sulfides fill fractures or form as sub- to euhedral grains associated with alteration phases replacing igneous silicates. None of the most common sulfide minerals, pyrite, pyrrhotite, pentlandite and chalcopyrite, are found exclusively as either an igneous sulfide or a secondary sulfide within Hole 735B.

Igneous Sulfides

Igneous sulfides in samples examined from alteration zones 2 through 5 commonly occur as monomineralic pyrrhotite or chalcopyrite, or assemblages of pyrrhotite ± chalcopyrite ± pentlandite [Figure 2] and are commonly surrounded by rims of smectite, iron-oxyhydroxide or calcite. The sulfide mineralogy observed for the igneous sulfides is similar to what has been described previously for primary igneous sulfides in Hole 735B (Alt and Anderson, 1991; Miller and Cervantes, 2002). In addition to these common mineralogies, rare ~100 μm subhedral grains displaying optical properties and chemical compositions approaching anomalous bornite ($Cu_{4.610}Fe_{0.935}S_{4.05}(Co_{0.001})$) and idaite ($Cu_{3.345}Fe_{1.194}S_4(Co_{0.021})(Ni_{0.023})$) with lamellae of chalcopyrite were observed in interstitial calcite in sample 177R-5, 61-66 cm, however these rare mineralogies are likely alteration products of primary igneous sulfides reacted with interstitial fluids.

In contrast to alteration zones 2 through 5, alteration zone 1 (lithologic unit VII) lacks the igneous pyrrhotite-chalcopyrite-pentlandite globules. The one sample from alteration zone 1 (lithologic unit VIII) that does contain igneous sulfides also contains rare ~20 x 55 µm anhedral interstitial greigite in smectite. The rare igneous sulfides are ≤ 20 µm porous pyrite globules. Rare ≤ 1 mm interstitial subhedral pyrite and pyrrhotite ± chalcopyrite grains displaying a similar porous texture were observed in sample 116R-3, 39-44 cm from alteration zone 2, but overall, porous igneous sulfides are uncommon in the low-temperature alteration zones 2 through 5.
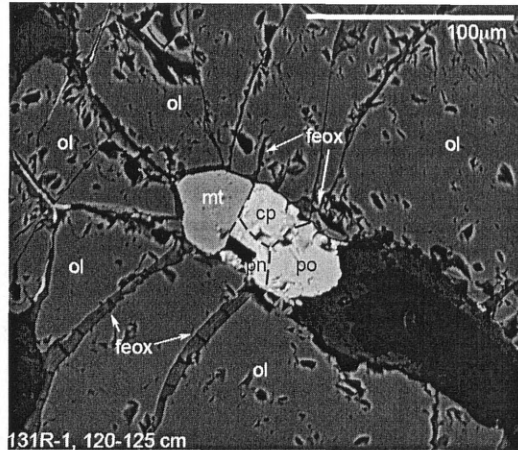
Figure 2. BSE image of igneous sulfide. cp=chalcopyrite, feox=iron oxyhydroxide, mt=magnetite, ol=olivine, po=pyrrhotite and pn=pentlandite. Dashed black lines added to highlight boundaries of phases within sulfide globule. Labeled sulfides were analyzed by microprobe.

Secondary Sulfides

The most common secondary sulfides in alteration zones 2 through 5 are part of an assemblage of smectite ± iron-oxyhydroxide ± calcite ± magnetite replacing olivine and clinopyroxene grains. This assemblage occurs as pseudomorphs of olivine and clinopyroxene commonly within 1 cm of 0.5 to 2 mm wide smectite ± calcite veins, or as a "mesh" texture among kernels of relict olivine and clinopyroxene in the host rock farther from the veins [Figures 3a & 3b]. Aggregations of secondary pyrite and pyrrhotite laths are commonly concentrated linearly within fractures of the "mesh" texture and along the inside edge of pseudomorphs within alteration zones 2 through 5. The pyrrhotite commonly displays a porous texture, and though both pyrite and pyrrhotite in these pseudomorphs may be present within the same sample, these two minerals never occur within the same replacement feature. Instead, mesh textures farther from veins host laths of well-crystallized to porous pyrrhotite whereas laths of pyrite occur in pseudomorphs closer the large smectite ± calcite veins, suggesting that pyrite has replaced pyrrhotite within the pseudomorph features. In alteration zone 1, olivine and clinopyroxene

replacements are abundant, but lack the associated secondary sulfide minerals common to alteration zones 2 through 5.

In addition to inclusions of sulfides within replacements of olivine and pyroxene, secondary sulfides also occur within major veins, interstitial areas, and fractures. Pyrite is the most common vein-associated secondary sulfide, present within calcite-smectite, smectite and zeolite veins [Figures 3c & 3d]. Commonly, the vein-associated pyrite is present as ≤ 5 μm sub- to euhedral grains in minor amounts, however, a large calcite vein in sample 107R-1, 81-86 cm hosts ~100 μm pyrite grains. Pyrite also fills fractures and occurs as sub- to euhedral blocky grains in interstitial areas within alteration zone 2. Additional secondary sulfides are uncommon, but are present as rare ~6 to 110 μm porous chalcopyrite ± trace ≤ 5μm globular chalcocite in smecitite-lined calcite veins [Figure 4a & 4b], and trace sub- to euhedral 100 x 35 μm chalcopyrite ± ≤ 40 μm globular pentlandite in interstitial smectite.
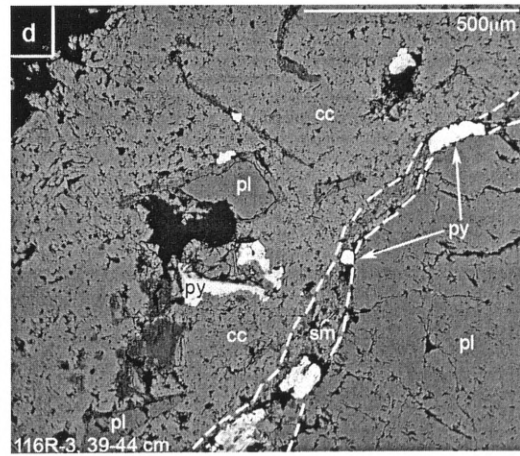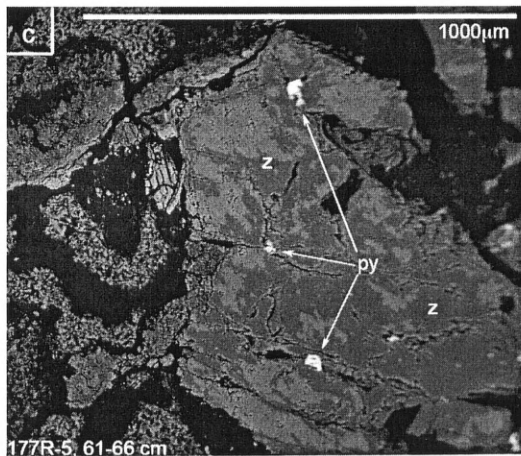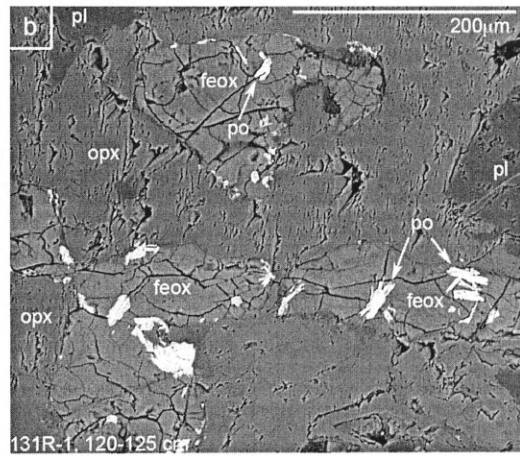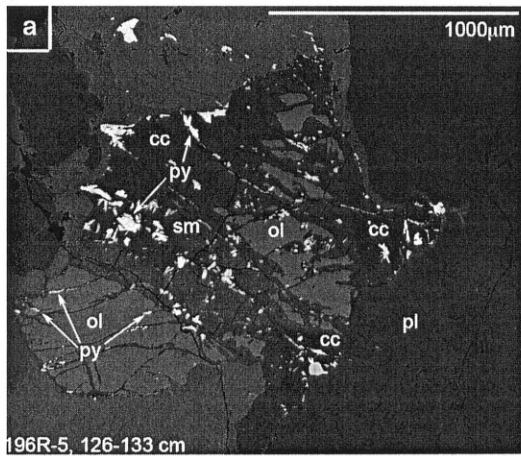
(Caption on the following page)

Figure 3. BSE Images of common secondary sulfides in Leg 176 samples. **a.** Mesh texture of calcite and smectite hosting aggregate of pyrite laths among kernels of relict olivine. **b.** Pyrrhotite laths in iron-oxyhydroxide pseudomorphs of olivine. **c.** Blocky pyrite grains in smectite-lined fractures of zeolite. **d.** Pyrite grains in calcite vein and associated smectite lining. Abbreviations: cc = calcite, feox = iron oxyhydroxide, ol = olivine, pl = plagioclase, po = pyrrhotite, py = pyrite, sm = smectite, z = zeolites. Labeled sulfides analyzed by microprobe.
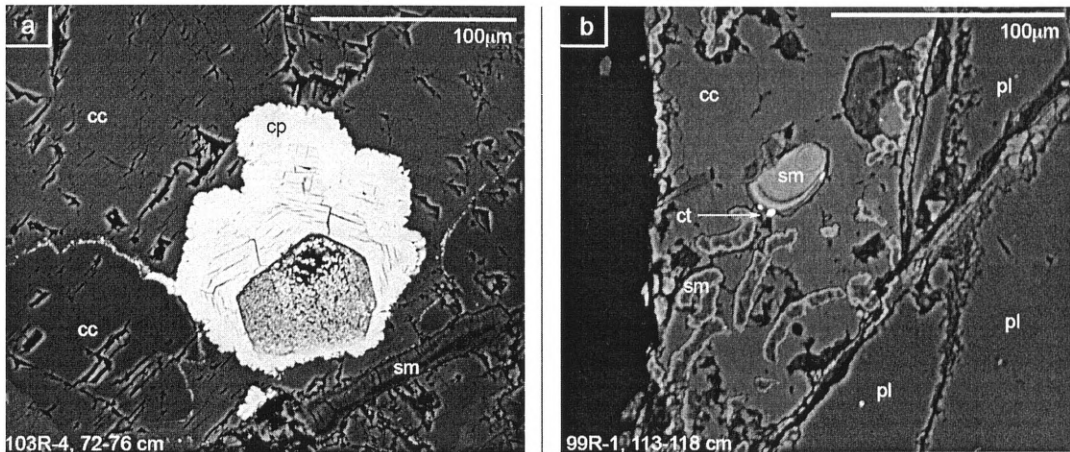
Figure 4. BSE images of rare secondary sulfides in Leg 176 samples. **a.** Porous cauliflower chalcopyrite with shrinkage cracks in a smectite-lined blocky calcite vein. **b.** Globular chalcocite in association with "vermicular" smectite within a blocky calcite vein. cc=calcite, cp=chalcopyrite, ct=chalcocite, sm=smectite and pl=plagioclase. Labeled sulfides analyzed by microprobe.

Sulfur Contents

Total sulfur contents of samples from this study range from 269 to 8305 ppm [Table 3]. The variation in total sulfur contents down-core correlates with the low-temperature alteration zones in agreement with previous results presented by (BACH et al., 2001) used to initially define the low-temperature alteration zones [Figure 5]. Sulfide sulfur (AVS + CRS) range from 85 to 8187 ppm with an average of 1933 ppm while sulfate sulfur ranges from 8-522 ppm with an average of 116 ppm. AVS contents range from ~0 (not detected) to 6123 ppm, with samples from alteration zone 4 encompassing nearly this full range in AVS contents whereas all other zones are limited to AVS contents less than 1000 ppm [Figure 6]. Sulfur in the CRS fraction ranges from 9 to 7564 ppm with alteration zones 2 and 4 accommodating significant portions of the overall range in CRS contents, while all other zones are limited to CRS contents below 200 ppm [Figure 6].

Figure 5. Profile of total sulfur contents for whole-rock samples from Hole 735B. Filled circles (●) = Leg 118 samples from Alt & Anderson (1991) [Appendix 3], filled triangles (▲) = Leg 176 "altered" samples from Bach et al. (2001), open triangles (△) = Leg 176 "fresh" samples from Bach et al. (2001), filled diamonds (◆) = Leg 176 single samples from this study, filled squares (■) = Leg 176 "highly-altered" sub-samples from this study, open squares (□) = Leg 176 "minimally-altered" sub-samples from this study. Black solid tie-lines connect "altered" and "minimally-altered" sub-sample pairs. Roman numerals denote lithologic stratigraphy as defined by Dick et al. (1991) and Shipboard Scientific Party (1999) [Table 1]. Dashed horizontal lines denote boundaries between low-temperature alteration zones as defined by Bach et al. (2001) [Table 2].

TABLE 3. Sulfur contents and isotopic compositions for whole-rock samples from the Leg 176 section of Hole 735B.

Lithologic Unit	Alteration Zone	Section, interval (cm)	Depth (mbsf)	S Contents (ppm)						δ³⁴S (‰)				
				AVS	CRS	Sulfide	Sulfate	Total	SO$_4$/ΣS	AVS	CRS	Sulfide	Sulfate	Total
VII		96R-1, 36-40	549.13	35	50	85	522	607	0.86	5.0	25.3	16.9	2.7	4.7
VII	1	99R-1, 113-118	567.24	---	113	113	183	296	0.62		0.7	0.7	13.6	8.7
VIII		103R-4, 72-76	599.87	170	185	355	60	415	0.14	0.6	2.7	1.7	-1.9	1.2
VIII		107R-1, 81-86	620.31	558	6576	7134	158	7292	0.02	8.7	16.9	16.3	9.0	16.1
IX		Minimally altered — 116R-3, 39-44	674.66	95	182	277	39	316	0.12	0.8	11.8	8.0	-4.8	6.4
IX		Halo & pyrite vein — 118R-1, 8-14	690.88	623	7564	8187	118	8305	0.01	8.4	9.8	9.7	2.0	9.6
X	2	Minimally altered — 127R-1, 105-109	765.95	555	1281	1836	68	1904	0.04	2.2	9.5	7.3	-1.2	7.0
X		Halo — 131R-1, 120-125	804.7	392	40	432	53	485	0.11	0.3	1.1	0.4	-0.9	0.2
X		Minimally altered — 133R-7, 107-111	832.33	580	2316	2896	92	2988	0.03	9.4	8.2	8.4	-2.1	8.1
X		Halo		997	520	1517	277	1794	0.15	6.7	5.5	6.3	3.9	5.9
X				684	9	693	48	741	0.06	4.4	4.0	4.4†	-3.6	3.9†
XI		140R-1, 119-124	881.49	160	31	191	166	357	0.46	1.8	-3.9	2.2	-5.6	-1.4
XI	3	150R-3, 56-62	973.12	321	39	360	58	418	0.14	-0.3	-2.3	-0.6	18.4	2.0
XI		159R-2, 74-80	1055.74	253	13	266	8	274	0.03	1.1	-2.3	0.9	-0.9	0.9
XI		168R-3, 59-64	1133.48	313	140	453	46	499	0.09	1.0	-1.5	0.0	-4.8	-0.5
XI	4	172R-7, 132-137	1178.13	66	4978	5044	38	5082	0.01	-1.2	2.5	-1.5	-8.0	-1.5
XI		177R-5, 61-66	1207.65	1521	38	1559	138	1697	0.08	5.7	2.1	5.6	-4.3	4.8
XI				254	257	511				3.3		2.7		
XI		181R-2, 7-13	1241.7	6123	1425	7548	209	7757	0.03	5.4	4.7	5.3	3.9	5.2
XII	5	196R-5, 126-132	1379.92	223	34	257	12	269	0.04	-0.8	-0.8	-0.8		
XII		202R-2, 135-141	1423.94	752	134	886	19	905	0.02	2.4	1.55	2.3	-5.7	2.1

Lithologic units as presented by Dick et al., (1991) and Shipboard Scientific Party (1999)

Alteration Zones as defined by Bach et al., 2001

--- = none detected

Blanks = not analyzed

Total* = sum of extracted sulfur from AVS, CRS and Sulfate extractions

Total** = (δ³⁴S$_{AVS}$ × AVS Contents/Σ Contents) + (δ³⁴S$_{CRS}$ × CRS Contents/ Σ Contents) + (δ³⁴S$_{SO4}$ × SO$_4$ Contents/ Σ Contents)

SO$_4$/ΣS = (Sulfate S Contents)/(Σ Contents)

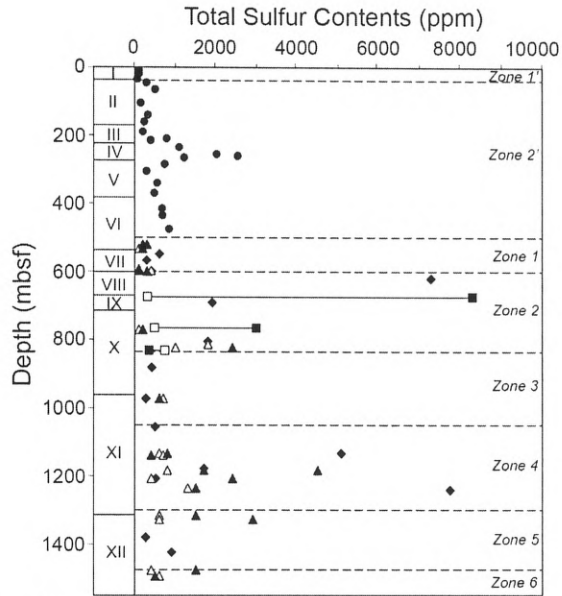† = Calculated by mass balance assuming δ³⁴S$_{CRS}$ = 4.8‰
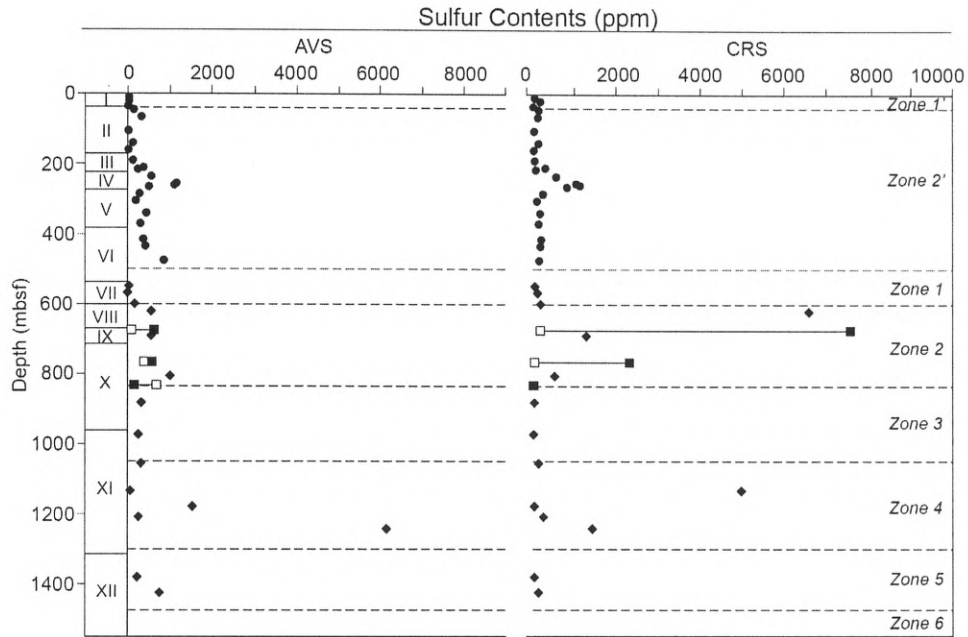
Figure 6. Profiles of AVS and CRS contents for whole-rock samples from Hole 735B. Filled circles (●) = Leg 118 samples from Alt & Anderson (1991) [Appendix 3], filled diamonds (◆) = Leg 176 single samples from this study, filled squares (■) = Leg 176 "highly-altered" sub-samples from this study, open squares (□) = Leg 176 "minimally-altered" sub-samples from this study. Black solid tie-lines connect "altered" and "minimally-altered" sub-sample pairs. Roman numerals denote lithologic stratigraphy as defined by Dick et al. (1991) and Shipboard Scientific Party (1999) [Table 1]. Dashed horizontal lines denote boundaries between low-temperature alteration zones as defined by Bach et al. (2001) [Table 2].

Sulfur Isotopes

Total $\delta^{34}S$ values ($\delta^{34}S_{Total}$) were calculated by mass balance according to equation 2 and range from -1.5 to 16.1‰ with an average of 6.4‰ [Table 3]. A similar mass balance calculation in reference to only AVS and CRS fractions was applied for determination of sulfide $\delta^{34}S$ values ($\delta^{34}S_{sulfide}$), which range from -1.5 to 16.9‰ [Table 3]. For $\delta^{34}S$ values measured on the separate sulfur fractions, $\delta^{34}S_{AVS}$ ranges from -1.2 to 9.4‰, $\delta^{34}S_{CRS}$ from -3.9 to 25.3‰ and $\delta^{34}S_{sulfate}$ from -8.0 to 18.4‰ [Table 3]. The general clustering of $\delta^{34}S_{AVS}$ and $\delta^{34}S_{CRS}$ values around $\delta^{34}S_{MORB}$ (0.1 ± 0.5‰ from Sakai et al., 1984) accompanied by some relatively enriched and depleted $\delta^{34}S$ values is similar to what has been described by Alt and Anderson (1991) for sulfur isotope measurements in the upper ~500 m of Hole 735B [Figure 7].

$$\delta^{34}S_{Total} = (\delta^{34}S_{AVS} \times \%AVS) + (\delta^{34}S_{CRS} \times \%CRS) + (\delta^{34}S_{Sulfate} \times \%Sulfate) \qquad (2)$$

Where:
$\delta^{34}S_n = \delta^{34}S$ of fraction "n"
$\%n$ = (sulfur contents of fraction "n")/(total sulfur contents)
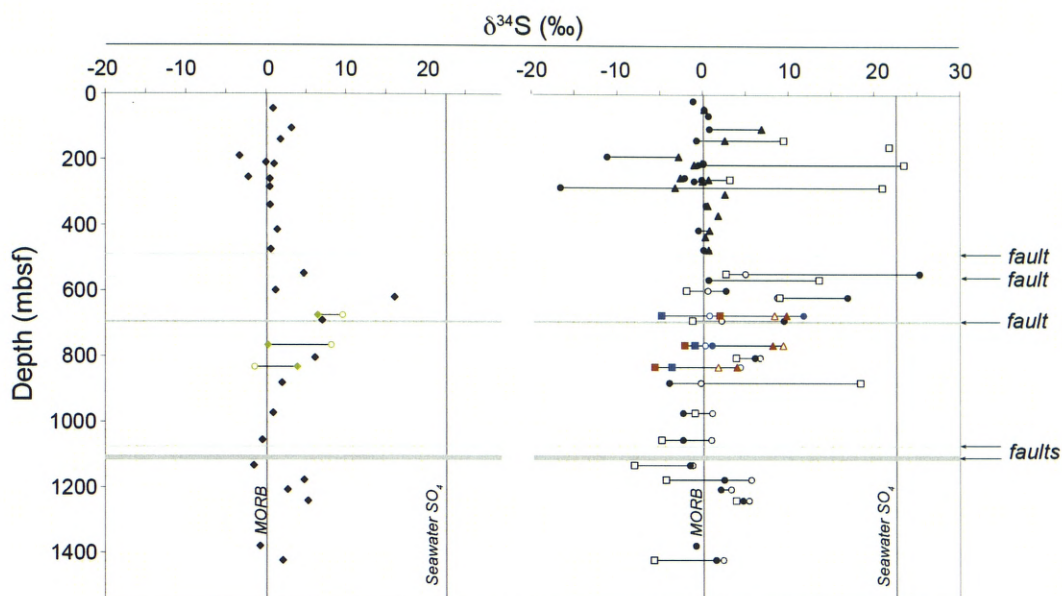
Figure 7. Sulfur isotope profiles for Hole 735B whole-rock samples. Left: Profile of $\delta^{34}S_{Total}$ where black filled diamonds (♦) = "single sample", green filled diamonds (♦) = "minimally altered" sub-sample and open green diamond (◇) = "highly altered" sub-sample. Right: Profile of $\delta^{34}S$ by fraction where filled triangles (▲) = AVS, filled circles (●) = CRS, open squares (□) = sulfate. Black symbols are "single samples" and colored symbols represent "minimally altered" and "highly altered" sub-sample pairs where brown symbols are "minimally-altered" sub-samples and blue symbols are "highly altered" sub-samples. Solid black tie-lines connect fractions of the same whole-rock sample. After Sakai et al. (1984) and Davis et al. (2003) $\delta^{34}S$ reference lines are drawn at 0.1‰ for MORB and 22.6‰ for seawater sulfate. Values of samples from upper 500 m as reported by Alt and Anderson (1991) [Appendix 3].

DISCUSSION

Alteration Effects

The range of total sulfur contents of samples from this study of 269 to 7757 ppm in comparison to the range of 100 to 1800 ppm for relatively unaltered samples from Leg 176 [Appendix 4] (Bach et al., 2001), indicates an overall addition of sulfur to the lower 1000 m of Hole 735B in response to alteration at temperatures ≤ 110°C. As the majority of "single samples" from this study have $SO_4/\Sigma S$ values of ≤ 0.15 [Table 3] and commonly host secondary sulfides, an accompanying addition of sulfide allowed for by reducing conditions is likely for most of the samples. Two sub-sample pairs have higher sulfide contents and lower $SO_4/\Sigma S$ values in the "highly altered" sub-samples than in their respectively paired "minimally altered" sub-samples, thereby supporting the interpretation of an overall addition of sulfur as sulfide minerals during low-temperature alteration. The only significant portion of the lower 1000 m of Hole 735B displaying low-temperature alteration which may not support an increase in sulfur contents by sulfide addition is the upper portion of alteration zone 1 (lithologic unit VII) where $SO_4/\Sigma S$ values of

> 0.60 indicate oxidative conditions [Table 3]. Sulfide was likely lost from alteration zone 1 through oxidation by seawater as illustrated by a decrease in sulfide sulfur contents accompanying an increase in oxidation state ($SO_4/\Sigma S$) between sub-samples of 133R-7, 107-111 cm.

Sulfur Exchange Mechanisms

        The net addition of sulfur to Hole 735B requires a sulfur source that was readily accessible to the material while it was being altered. According to $\delta^{18}O$ and δD analyses, the high temperature hydrothermal fluids involved in the alteration of gabbros in Hole 735B include magmatic and seawater components (Alt and Bach, 2006). As magmatic fluids can host sulfur transported from depth and ambient seawater contains ~900 ppm of sulfur as dissolved sulfate (Ohmoto and Goldhaber, 1997), either of these fluid components may act as sources of sulfur into the system. High-temperature hydrothermal fluids ($250^{o}C$ to $380^{o}C$) host mixtures of H_2S from reacted igneous sulfides and seawater sulfate (Alt, 1995b), and may also act a source of sulfur to Hole 735B. However, the samples used in this study host smectite, carbonate and zeolite as major veins in addition to iron-oxyhydroxide, as predominant alteration minerals. These vein minerals have all been interpreted as low-temperature alteration products from infiltrating seawater along late-stage brittle fractures based on $^{87}Sr/^{86}Sr$, $\delta^{18}O$, and $\delta^{13}C$ values and Sr contents of vein minerals and whole rocks (Alt and Bach, 2001; Bach et al., 2001). As samples containing other vein minerals were either avoided during sample selection, or removed from the sample prior to processing, seawater sulfate is taken to be the source reservoir responsible for the addition of sulfur observed in this study.

Sulfide Addition by Microbial Sulfate Reduction

        As the secondary mineralogy and geochemistry indicate sulfur addition in the form of sulfide minerals, a reducing mechanism is required in order to have transferred the sulfur from the dissolved seawater sulfate into a form of sulfide available for sulfide precipitation. Inorganic sulfate reduction and thermochemical sulfate reduction are not applicable to the production of alteration effects observed in our samples because they are kinetically inhibited below $150^{o}C$ and $200^{o}C$, respectively, when only pathways that involve reductants available in sub-seafloor basement environments are considered (Goldstein and Aizenshtat, 1994; Malinin and Khitarov, 1969; Ohmoto and Goldhaber, 1997; Ohmoto and Lasage, 1982). However, microbial sulfate reduction can occur from -1.5 to $110^{o}C$ (Canfield, 2001; Jørgensen et al., 1992), and thus, it is the only reasonable sulfate reducing mechanism to produce sulfide within the $10^{o}C$ to $110^{o}C$ range of alteration temperatures described by our samples. Though there are viable chemical pathways by which thermochemical sulfate reduction may also operate at these temperatures, such processes require the presence of pre-existing H_2S and hydrocarbons to catalyze reduction

reactions (Goldstein and Zizenshtat, 1994; Ohmoto and Goldhaber, 1997). Such conditions are readily available within oil-fields where low-temperature thermochemical sulfate reduction has been suggested to take place, but within submarine basement environments, abundant hydrocarbons are not present, thereby discounting this as a viable mechanism in Hole 735B.

Though microbial sulfate reduction does not directly form iron-sulfide minerals (equation 3.1 and 3.2), the signature of this process in the mediation of sulfide mineral formation is recorded in the $\delta^{34}S$ value of sulfide minerals. At equilibrium, SO_4 is enriched in ^{34}S relative to coexisting H_2S. Microbial sulfate reduction however, imparts a kinetic isotope fractionation primarily due to the biological preference for processing the weaker S-O bond formed with ^{32}S versus ^{34}S. (Ohmoto and Goldhaber, 1997) The total degree of fractionation imparted by sulfate reducers between SO_4 and H_2S can vary significantly due to temperature, rate of reduction, electron donor and the specific species of sulfate reducer involved, and has been described by enrichment factors of $\epsilon_{SO4-H2S} \leq 45$‰ in natural samples (where $\epsilon_{SO4-H2S} = \delta^{34}S_{SO4} - \delta^{34}S_{H2S}$) (Canfield, 2001). Upon contact of H_2S with Fe^{2+} in solution, sulfide minerals readily precipitate with minimal fractionation of sulfur isotopes under the conditions of low fO_2 and low pH assumed to be present during sulfate reduction in Hole 735B (see "Iron-silicate Replacements and Secondary Sulfide Formation"), thereby producing sulfide minerals with $\delta^{34}S$ values that are nearly identical to that of the H_2S (Ohmoto and Rye, 1979). Samples from this study have $\epsilon_{SO4-sulfide}$ values ranging from 4.2 to 30.6‰ in reference to $\delta^{34}S_{SO4}$ of 22.6‰ for seawater (Davis et al., 2003), which is consistent with isotope fractionation imposed by microbial sulfate reduction. Sulfur isotope data presented by Alt and Anderson (1991) for Leg 118 samples gives $\epsilon_{SO4-sulfide}$ values of 14.9 to 42.4‰. These data were interpreted in terms of hydrothermal processes and low-temperature oxidation effects, but are also consistent with microbial sulfate reduction. By comparison, marine sedimentary pyrites produced by microbial sulfate reduction pathways display a range in $\epsilon_{SO4-sulfide}$ of 24 to 71‰ with an average of 51‰ (Canfield and Teske, 1996). The relatively small enrichment factors described in Hole 735B in respect to marine sedimentary pyrites may be due to a combination of factors including higher temperatures of reaction within Hole 735B, the involvement of different species of sulfate reducers, a greater utilization of H_2 in lieu of organic carbon as an electron donor in basement environments, and reservoir effects (Canfield, 2001; Kaplan and Rittenberg, 1964).

$$SO_4^{2-} + 2CH_2O \rightarrow H_2S + 2HCO_3^- \qquad (3.1)$$
$$2H^+ + SO_4^{2-} + 4H_2 \rightarrow H_2S + 4H_2O \qquad (3.2)$$
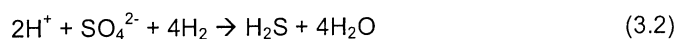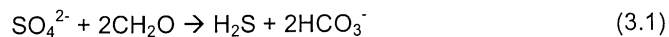
During subseafloor hydrothermal alteration, the supply of dissolved sulfate to a specific location within the hydrothermal system may become limited due to decreasing permeability or to

sulfate reduction occurring upstream, or from changes in the balance of sulfate reduction versus sulfide oxidation within the specific area of interest. Once the rate of incoming sulfate reaches levels equal to, or less than the rate of sulfate reduction, the system is considered to be locally "closed" to sulfate (Ohmoto and Goldhaber, 1997). The effects of closure to sulfate during reduction processes in Hole 735B are two-fold. Firstly, the amount of additional sulfur that may be precipitated as sulfide minerals is limited to the concentration of dissolved sulfate present upon closure of the system, which presumably would be a maximum of ~900 ppm based on the concentration of dissolved sulfate available in seawater and a water-to-rock ratio equal to 1. Secondly, as a consequence of the finite supply of remaining sulfate within the local system, rayleigh processes result in a progressive enrichment in ^{34}S within the dissolved sulfate reservoir as microbial sulfate reduction continually removes ^{32}S for the production of H_2S [Figure 8]. Because the sulfate reservoir from which the H_2S is formed continually becomes heavier, each reduction step imposed by the sulfate reducers produces progressively heavier H_2S. If Fe^{2+} is available in solution, then H_2S can be precipitated as a sulfide mineral thereby preventing a back-reaction to SO_4^{2-} and allowing for considerable increases in the $\delta^{34}S$ of the individual precipitated sulfide minerals beyond that of the original seawater sulfate reservoir.
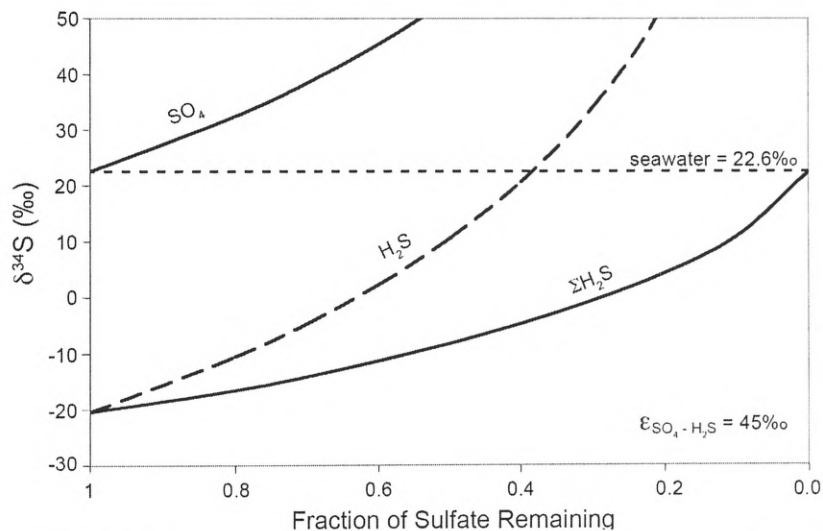
Figure 8. Closed-system microbial sulfate reduction fractionation model. Through rayleigh processes, the $\delta^{34}S$ of actively precipitated evolved sulfide can increase beyond the original $\delta^{34}S$ of the initial seawater sulfate. Curved lines express $\delta^{34}S$ for species within the system at fractionation progress = "f" where SO_4^{2-} = seawater sulfate, H_2S = hydrogen sulfide in a system with active precipitation of sulfide and ΣH_2S = H_2S in a system closed to precipitation of sulfide until after all sulfate has been reduced. Straight dashed line represents $\delta^{34}S$ of initial seawater sulfate (Davis et al., 2003). Fractionation model based on maximum known isotopic enrichment factor (ε) imparted by sulfate reducers of 45‰ (Canfield, 2001) and rayleigh fractionation equations as described by Ohmoto and Goldhaber (1997).

The 735B samples can be compared to open and closed-system microbial sulfate reduction models as shown in Figure 9. In these models, a reference unaltered gabbro is also plotted as $\delta^{34}S_{sulfide}$ = 0.1‰ based on the $\delta^{34}S$ of fresh MORB (Sakai et al., 1984), and at sulfide contents of 600 ± 433 (1σ) ppm based on the average sulfur contents of "fresh" gabbro samples from Leg 176 [Appendix 4] (Bach et al., 2001). Samples from this study have $\delta^{34}S_{sulfide}$ values that are both greater and less than the unaltered gabbro. Some samples display a tight scatter about the fresh gabbro $\delta^{34}S_{sulfide}$ value and are within the range of the fresh gabbro sulfide sulfur contents, whereas others exhibit a broad, positive skew to higher $\delta^{34}S_{sulfide}$ values and sulfide sulfur contents. The observed slightly negative $\delta^{34}S_{sulfide}$ values can be achieved by reduction in an open system which allows for the negative fractionation imposed by sulfate reducers to be reflected in precipitated sulfide minerals. Meanwhile, the general positive trend of $\delta^{34}S_{sulfide}$ with increasing sulfide sulfur contents requires reduction in a closed-system in order to produce increasingly positive values by microbial reduction of seawater sulfate. However, some of the samples displaying the greatest $\delta^{34}S_{sulfide}$ values also display gains in sulfur that are in excess of the 900 ppm that can be supplied by seawater sulfate in a closed system (at a water-to-rock ratio of 1), thereby suggesting the involvement of an earlier period of open-system reduction as shown in Figure 9, and that local systems evolved in terms of the supply of dissolved sulfate.
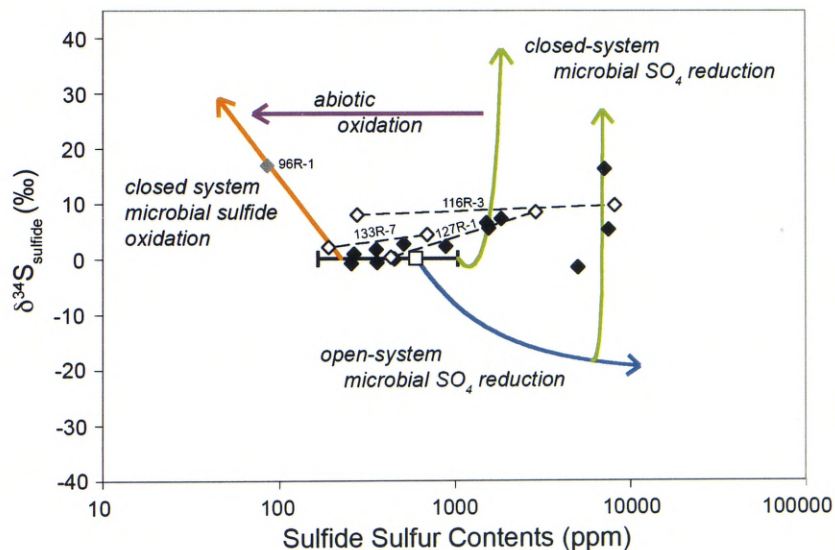
Figure 9. Mechanisms affecting sulfur geochemistry of 176 samples at low-temperature. Addition of sulfide to fresh gabbro (600 ± 433 ppm) through closed and open-system microbial sulfate reduction calculated based on $\varepsilon_{SO4-H2S}$ = 45‰ (CANFIELD, 2001), initial seawater sulfate $\delta^{34}S$ = 22.6‰ (Davis et al., 2003) and a concentration of 28 mmol/kg (Pilson, 1998). Evolution of sulfide addition pathways illustrated by addition of sulfide through open-system sulfate reduction followed by sulfide addition through closed-system sulfate reduction. Loss of sulfide from fresh gabbro (600 ± 433 ppm) by closed system microbial sulfide oxidation calculated based on $\varepsilon_{H2S-SO4}$ = 18‰ (Canfield, 2001). Abiotic oxidation results in no sulfur isotope fractionation (Ohmoto and Goldhaber, 1997). Evolution of sulfide loss may include components of abiotic or closed-system

microbial sulfide oxidation pathways. Black diamonds (♦) = single-samples with $SO_4/\Sigma S$ < 0.16, grey diamond (◈) = single-sample with $SO_4/\Sigma S$ > 0.45 and open diamonds (◇) = paired highly- and minimally-altered sub-sample. White square (□) = estimate of unaltered gabbro from Hole 735B with $\delta^{34}S_{sulfide}$ = 0.1‰ (SAKAI et al., 1984) and sulfide sulfur contents = 600 ± 430 (1σ) ppm calculated from the average sulfur contents of "fresh" samples from Leg 176 presented by Bach et al. (2001).

Sulfide Loss by Oxidation

A loss of sulfide under low-temperature conditions in the sub-sample pair 133R-7, 107-111 cm suggests that oxidation resulted in the removal of sulfide from discrete areas of Hole 735B. Oxidation of sulfides within submarine environments can occur readily at low-temperatures via abiotic oxidation by dissolved oxygen (O_2) (Ohmoto and Goldhaber, 1997) or by oxidation by sulfide oxidizing microorganisms (Canfield, 2001; Wirsen et al., 1998, Wirsen et al., 1993). Abiotic oxidation of sulfide by O_2 does not fractionate sulfur isotopes, whereas the biological preference for processing ^{32}S imposes kinetic fractionations during microbial sulfide oxidation with $\varepsilon_{H2S-SO4}$ ranging from 10 to 18‰ from direct oxidation pathways, and more variable fractionations when intermediate steps are involved (where $\varepsilon_{H2S-SO4} = \delta^{34}S_{H2S} - \delta^{34}S_{SO4}$) (Canfield, 2001). Thus, while both abiotic and biotic oxidation processes result in a loss of sulfide (increasing $SO_4/\Sigma S$), microbial sulfide oxidation also enriches the remaining sulfide minerals in ^{34}S. In terms of sulfide oxidation, the system can become closed if simultaneous production of H_2S by microbial sulfate reduction is inhibited or operates at rates below or equal to the rate of sulfide oxidation. In such scenarios, progressive enrichments in ^{34}S occur within the remaining sulfide minerals with increasing degrees of sulfide oxidation (Canfield, 2001; Ohmoto and Goldhaber, 1997). The progressive ^{34}S enrichments in the remaining sulfide mineral due to rayleigh processes can thereby lead to elevated $\delta^{34}S$ values of reacted sulfide minerals relative to the $\delta^{34}S$ value of the sulfide mineral prior to oxidation [Figure 10]. The alteration of 133R-7, 107-111 cm may have included a component of abiotic oxidation to result in a loss of sulfide in the highly altered sub-sample, however the elevated $\delta^{34}S_{suflide}$ in both of the sub-samples requires the involvement of microbial oxidation processes, or a phase of microbial sulfate reduction.
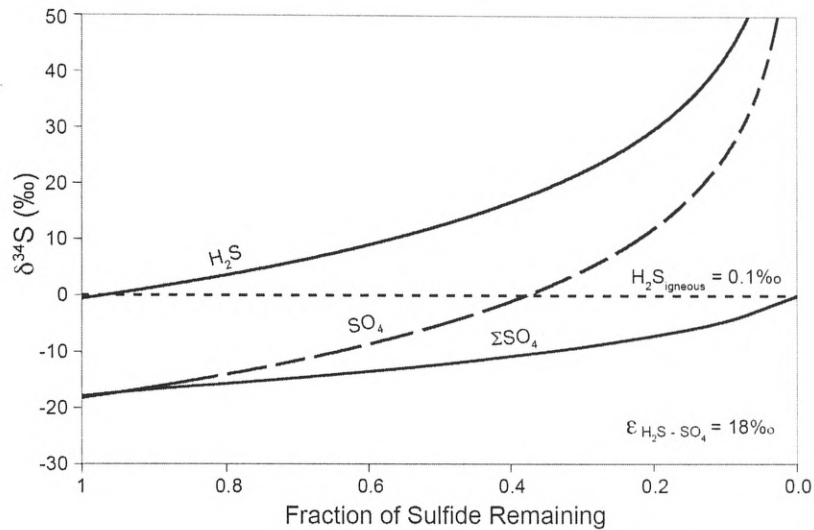
Figure 10. Closed-system microbial sulfide oxidation fractionation model. Through rayleigh processes, the $\delta^{34}S$ of the remaining sulfide mineral, plotted as H_2S, increases with continuing degrees of fractionation. Curved lines express $\delta^{34}S$ for species within the system at fractionation progress = "f" where H_2S = remaining sulfide species, SO_4 = derived sulfate, and ΣSO_4 = cumulative derived sulfate. Straight dashed line represents initial $\delta^{34}S$ of igneous sulfide (Sakai et al., 1984). Fractionation model based on maximum known isotopic enrichment factor (ε) imparted by sulfate oxidizers of 18‰ (Canfield, 2001) and rayleigh fractionation equations as described by Ohmoto and Goldhaber (1997).

Sample 96R-1, 36-40 cm is highly oxidized ($SO_4/\Sigma S = 0.86$), has low sulfide contents (85 ppm), lacks secondary sulfides, contains rare porous igneous sulfides and trace sulfide globules, and has a high $\delta^{34}S_{sulfide}$ value (16.9 ‰) [Table 3]. These points suggest the involvement of microbial oxidization of igneous sulfides under closed-system conditions [Figure 9]. The minimally altered sub-samples of 116R-3, 39-44 cm lacks secondary sulfides, so the elevated $\delta^{34}S_{sulfide}$ value (8.0 ‰) may also reflect microbial oxidation processes. The evidence for these pathways suggests the involvement of microbial sulfide oxidation that is independent of, or precedes microbial sulfate reduction. Overall, these various pathways indicate the complexity of the system: there is a component of closed-system microbial processes present in all oxidized samples; microbial sulfide oxidation occurred prior to reduction processes in some samples; and microbial sulfate reduction occurred prior to or during oxidative alteration in other samples.

Sulfate-Sulfide Disequilibrium

Most samples from this study have $\delta^{34}S_{Sulfide}$ values greater than the $\delta^{34}S_{SO4}$ for fractions recovered from the same sample [Figure 11]. This is opposite to the expected relationship for co-existing sulfur species produced under equilibrium conditions whereby species with higher oxidation states should have higher $\delta^{34}S_{Sulfide}$ values (Ohmoto and Goldhaber, 1997). This

20

sulfate-sulfide disequilibrium is consistent with kinetic fractionation produced by microbial processes.
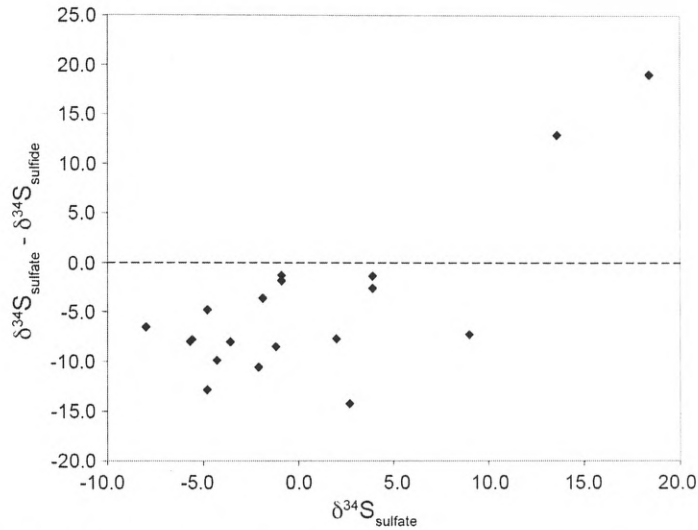
Figure 11. Fractionation between sulfate and sulfide versus $\delta^{34}S_{sulfate}$ for Leg 176 samples. Most samples have $\delta^{34}S_{sulfide} > \delta^{34}S_{SO4}$ suggesting a kinetic fractionation during alteration, perhaps via microbial pathways.

Textural Evidence of Microbial Involvement?

Rare vermiform smectite associated with carbonate and zeolite veins in alteration zones 1 and 3 [Figure 4b] is texturally similar to proposed smectitic bacteriomorphs in the Columbia River Basalts (McKinley et al., 2000; Thomas-Keprta et al., 1998) and basaltic martian meteorite ALH84001 (Thomas-Keprta et al., 1998). Though several orders of magnitude greater than either of these previously reported bacteriomorphs, the 5 to 50 μm vermicular smectite features in Hole 735B are comparable in size to large sulfide oxidizers isolated from seafloor environments (Schulz and Jørgensen, 2001), thereby suggesting that these features may be mineralized sulfide oxidizers. Associated microbial sulfide reduction is indicated by the occurrence of porous igneous sulfides and trace globular sulfides within the vermicular smectites, thereby lending further support to this proposed paragenesis

Based on textural and size evidence alone, an inorganic origin for the vermicular smectite features in 735B is equally possible. Vermiform textures in clays have been produced in hydrothermal alteration experiments above 150°C (Small et al., 1992), which verifies the abiotic origin of the experimentally-produced texture based on the instant degradation of adenosine triphosphate (ATP) at these temperatures (Madigan and Martinko, 2006). Furthermore, vermiform textures in smectite can also form during the drying of geologic samples in air (Velbel

and Barker, 2008), however, this drying effect is unlikely to be responsible for the vermiform textures observed in Hole 735B as they are enclosed in calcite.

Iron-silicate Replacements and Secondary Sulfide Precipitation

Elevated Fe^{3+}/Fe_{total} values in altered Leg 176 samples (Bach et al., 2001) and the common association of magnetite ($FeO \cdot Fe_2O_3$) within replacements of olivine and pyroxene (Alt and Anderson, 1991; Bach et al., 2001) demonstrate localized oxidation of iron silicate minerals throughout Hole 735B which may have produced H_2 by reduction of H_2O (Stevens and McKinley, 2000). As lithotrophic sulfate reducers utilize H_2 as an electron donor (Canfield, 2001; Edwards et al., 2005), the involvement of an H_2-forming reaction may have allowed for the initial establishment of sulfate reducers within Hole 735B, similar to the processes suggested by Stevens and Mckinley for the support of autotrophic metabolisms in the Columbia River Basalts (1995). With progressive reaction progress, the reduction and acidification of fluids (equation 4.1 and equation 4.2) may also allow Fe^{2+} to become available in solution (equation 4.3) thereby promoting the precipitation of sulfide minerals in the presence of H_2S provided by sulfate reducers.

$$2Fe_2SiO_4 + H_2O + O^{2-} \rightarrow 2Fe_2O_3 + H_2O + H^+ + SiO_2 + H_2^o \qquad (4.1)$$

$$2Fe_2SiO_4 + 2H_2O \rightarrow FeO \cdot Fe_2O_3 + H^+ + 2SiO_2 + FeO(OH) + H_2^o \qquad (4.2)$$

$$2Fe_2SiO_4 + 2H^+ \rightarrow FeO \cdot Fe_2O_3 + 2SiO_2 + Fe^{2+} + H_2^o \qquad (4.3)$$
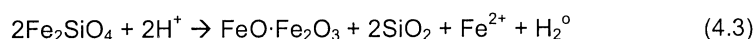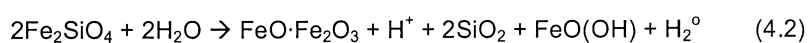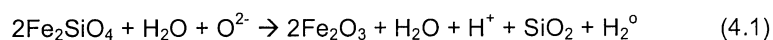
The lath morphology displayed by all secondary sulfides associated with replacement features of olivine and clinopyroxene suggests initial precipitation of these secondary sulfides as pyrrhotite, which would be expected for these samples irrespective of sulfur fugacity due to the high nucleation barrier for pyrite with respect to monosulfides at temperatures less than 100^oC (Schoonen and Barnes, 1991). Transformation of pyrrhotite to pyrite to produce the observed pyrite laths can occur by addition of S^{2-} via sulfidation, or Fe^{2+} loss by oxidation (Belzile et al., 2004, Schoonen and Barnes, 1991). Sulfidation would be a possible mechanism for pyrite formation based on the production of H_2S by sulfate reduction, however, the occurrence of porous pyrrhotite between well-crystallized pyrrhotite and lath-shaped pyrite within the sulfide mineral zonations surrounding low-temperature alteration veins suggests that the pyrrhotite to pyrite transformation in Hole 735B is the result of pyrrhotite oxidation. The lath morphology retained by the pyrite is not a characteristic morphology resulting from pyrrhotite oxidation by microbial oxidation (Bhatti et al., 1993), suggesting that abiotic oxidation caused the transformation of pyrrhotite to pyrite. Abiotic oxidation of pyrrhotite requires the presence of O_2 in solution (Knipe et al., 1995), which within highly reacted areas, may have occurred locally as altering iron silicates became depleted in iron, thereby lowering the local reduction potential and allowing for incoming seawater to retain O_2 in solution longer. According to the experimental

model by Pratt et al. (1994), a progressive oxidation of pyrrhotite by O_2 would lead to the production of increasing Fe^{2+} deficiency in iron sulfides towards the main O_2 source, similar to that in the sulfide mineral gradients in wallrock adjacent to veins in Hole 735B. A gradient in relative abundance of pyrrhotite and pyrite also exists vertically as shown by the AVS and CRS profiles [Figure 6] as well as in observed sulfide mineralogy, whereby pyrite is abundant in alteration zone 2, common in alteration zone 3, and is generally lacking within alteration zones 4 and 5 [Appendix 2]. Though sulfur is also oxidized during the oxidation of pyrrhotite, the temporary formation of pyrite is allowable due to stoichiometric relationships which result in the oxidation of only 1 mole of sulfur for every 8 moles of iron that is oxidized (Bach and Edwards, 2003).

A caveat to this proposed mechanism is that because all sulfide reducers are obligate anaerobes (Canfield, 2001), the water involved in the initial oxidation of iron silicates must be depleted in O_2 in order to support microbial sulfate reduction. Hematite lamellae within magnetite in olivine and clinopyroxene pseudomorphs in alteration zone 1 reflect the presence of O_2 within alteration fluids in this zone, which is likely the factor that prohibited the formation of secondary sulfides in this zone. The O_2 present in alteration zone 1 was likely from oxygenated seawater introduced through a porous fault in the middle of this alteration zone at 560 mbsf (Dick et al., 2000). Reaction of these fluids in alteration zone 1 would have eventually removed O_2 from solution, thereby allowing for the establishment of microbial sulfate reducers down-flow from alteration zone 1, possibly within the deeper alteration zones. However, the reduction potential of reacted iron silicates is exhausted with increased reduction progress (Bach and Edwards, 2003) and advance of the oxidation front, potentially making the presence of sulfate reducers temporary.

SUMMARY & CONCLUSIONS

The results of this study provide evidence for the interactions of microbial sulfate reduction, microbial sulfide oxidation, and abiotic oxidation during low-temperature alteration of lower oceanic crust gabbros in Hole 735B.

Secondary sulfides in the lower 1000 m of Hole 735B are common throughout low-temperature alteration zones 2 through 5 as aggregations of pyrrhotite and pyrite laths in assemblages of smectite ± iron-oxyhydroxide ± magnetite ± calcite replacing olivine and clinopyroxene adjacent to 0.5 to 2 mm veins of smectite ± calcite. Additional secondary pyrite also occurs locally in minor abundances within smectite ± calcite and zeolite veins. As primary igneous globules of pyrrhotite ± chalcopyrite ± pentlandite are still present, and total sulfide contents for most samples are within or above the range of 600 ± 433 (1σ) ppm sulfur assumed for fresh gabbro in Hole 735B (Bach et al., 2001), the observed secondary sulfides are interpreted

as additions of sulfur to the gabbroic material from exchange with seawater sulfate. Microbial sulfate reduction is the only viable exchange mechanism due to sample selection based on the presence of associated vein minerals with formation temperatures $\leq 110^{o}$C, and was likely enabled by the production of H_2 from the oxidation of associated olivine and pyroxene grains. Among relatively reduced samples ($SO_4/\Sigma S \leq 0.15$), a wide range in $\delta^{34}S_{sulfide}$ values from -1.5 to 16.3‰ and sulfide additions ranging up to values greater than 900 ppm between associated sub-samples indicates the involvement of both open and closed system processes during reduction. An evolution towards locally closed systems may have eventually limited the amount of sulfide that was added to Hole 735B during low-temperature alteration.

Evidence for biotic and abiotic oxidation within Hole 735B indicate additional limitations imposed on the net addition of sulfide during low temperature alteration. The involvement of microbial sulfide oxidation within Hole 735B is evident in some highly oxidized samples ($SO_4/\Sigma S \geq 0.46$) by low sulfur contents, high $\delta^{34}S_{sulfide}$ values, porous igneous sulfides, globular secondary sulfides and a lack of the secondary sulfides commonly associated with olivine and clinopyroxene replacement features. The extent of the microbially-driven oxidation is unclear as co-existence of sulfide oxidizers with sulfate reducers may have masked the effects by which sulfide oxidation can be identified but has clearly led to a decrease in sulfide sulfur in some samples. Additional oxidation by late-stage penetration of oxygenated fluids throughout low-temperature alteration zones 2 and 3 may have resulted in some loss of sulfides, but most clearly influences sulfide contents by the formation of environments that are inhospitable to sulfate reducers, thereby preventing any additional formation of secondary sulfide once an oxygenated environment is locally established.

The amount of sulfide that was precipitated during low-temperature alteration may have been limited by the development of closed system reduction processes in addition to oxidation by sulfide oxidizers and late-stage penetration of oxygenated seawater. Nonetheless, microbial interactions within the lower 1000 m of Hole 735B resulted in a net addition of sulfur and an elevation of the average $\delta^{34}S_{Total}$ to 6.4‰ within focused areas altered at temperature $\leq 110^{o}$C. Similar microbial processes may have also influenced the fractionation of sulfur isotopes during low-temperature alteration in the upper ~500 m. These results indicate that exposed lower oceanic crust can locally serve as a sink for sulfur, and may harbor measurable localized enrichments in ^{34}S due to interactions with microorganisms.

APPENDIX 1. Detailed Sulfur Extraction Procedures

Figure A.1.1 illustrates the procedure followed for the extraction of sulfur from powdered whole-rock samples. This procedure is a synthesis of published extraction methods for acid volatile sulfides (AVS), chromium reduced sulfides (CRS), and sulfates, which target predominately monosulfides (pyrrhotite, pentlandite, greigite, and chalcocite), disulphides (elemental sulfur and pyrite) and sulfates (organic and inorganic), respectively, via chemical digestion of sample material. All three digestions were carried out in succession on each sample using an apparatus modified from those utilized by previous investigators [figure A.1.2]. By completing all digestions in this manner within a single vessel, tedious time-consuming filtration steps between digestions as required by the original methods (Rice et al., 1993; Tuttle et al., 1986; Zhabina and Volkov, 1978) were avoided, which serendipitously eliminated errors associated with accidental oxidation or loss of sample between collection of separate sulfur fractions.
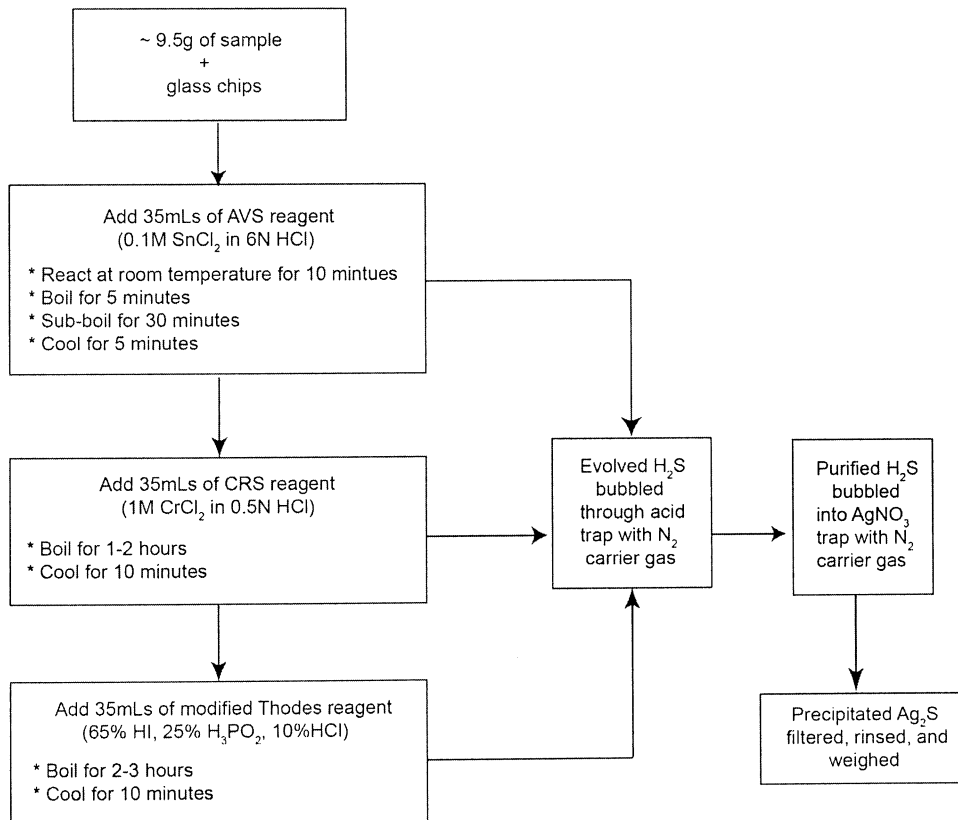
Figure A.1.1. Flow chart of sulfur extraction procedures.
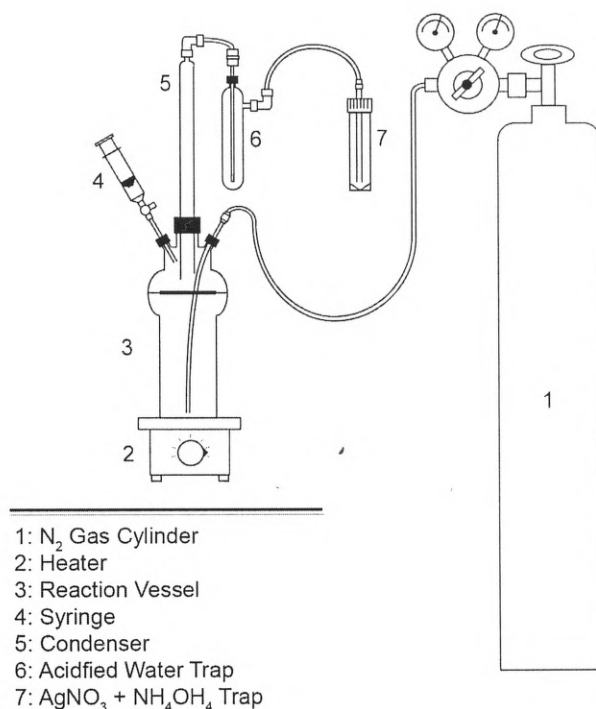
Figure A.1.2. Apparatus used for sulfur extractions.

1: N$_2$ Gas Cylinder
2: Heater
3: Reaction Vessel
4: Syringe
5: Condenser
6: Acidfied Water Trap
7: AgNO$_3$ + NH$_4$OH$_4$ Trap

The total sulfur extracted according to these procedures may not include the total sulfur present in the sample. Although all inorganic sulfur and organic sulfate is recoverable (Pepkowitz and Shirley, 1951), none of the reagents utilized in this procedure have been shown to be capable of digesting carbon-bonded sulfur (Canfield et al., 1986; Pepkowitz and Shirley, 1951), which is the form of sulfur present in principal amino acids such as cysteine and methionine (Shan and Chen, 1995).

General Overview and System Set-up

For each sample, ~ 9.5g of powdered rock (weighed to 0.1 mg) was placed in a reaction vessel atop a hotplate, as successful extraction of the AVS, CRS and sulfate fractions using each of the prescribed procedures requires boiling (Canfield et al., 1986; Rice et al., 1993; Thode et al., 1961). Because water vapor may be produced during boiling, a condenser was attached to the top of the reaction vessel to trap any evolved water vapor, thereby preventing its movement through the system. Also attached to the reaction vessel was a tube supplying a continuous flow of pre-purified nitrogen (N$_2$) gas into the bottom of the reaction vessel. The continuous supply of N$_2$ established an inert atmosphere within the reaction vessel and served as a carrier gas to transport any volatiles evolved from the digestions. A second tube inserted into the top of the

reaction vessel was attached to a three-way valve to be used in conjunction with 60 cc syringes for the introduction of reagents into the reaction vessel with minimal introduction of ambient air.

Where sulfur is present in the targeted species, each digestion results in the production of H_2S from that species, as well as possibly Cl^- due to the presence of hydrochloric acid (HCl) in each of the reagents. Transport of Cl^- through the system is problematic as precipitation of Cl^- in the end trap of the system leads to an overestimation of sulfur contents and can lead to isobaric interferences during isotopic analysis of the combusted precipitate. Thus, an in-line acidified water trap (DD water + nitric acid) was placed after the condenser to strip Cl^- from the gas stream (Backlund et al., 2005). This purified gas stream was then bubbled into a sterile centrifuge tube containing ~34 mLs of a 0.2 M silver nitrate ($AgNO_3$) in 10% ammonium hydroxide (NH_4OH) solution via a tube inserted through its cap. The solution in this "$AgNO_3$ trap" allowed for any H_2S present in the gas stream to precipitate evolved sulfur as silver sulfide (Ag_2S) while preventing precipitation of any remaining Cl^- present in the gas stream to AgCl by complexation of ammonia with Ag^+ (equation a.1.1 and equation a.1.2). Thode (1961) applied a post-extraction NH_4OH rinse to the precipitates formed in a trap solution containing only $AgNO_3$, however modification of the $AgNO_3$ solution itself simplifies this purification step by preventing the initial precipitation of the AgCl. Additionally, alteration of the $AgNO_3$ solution in such a manner buffers the trap solution to ammonium nitrate (NH_4NO_3) by reaction of NH_4OH with any nitric acid (HNO_3) produced as a byproduct of the Ag_2S-forming reaction (equations. a.1.1 and a.1.3) (Snoeyink and Jenkins, 1980) thereby preventing the oxidation and exhaustion of the $AgNO_3$ trap solution by HNO_3.

$$H_2S + AgNO_3 \rightarrow Ag_2S + HNO_3 + H^+ \qquad (a.1.1)$$
$$Cl^- + AgNO_3 + 2NH_4OH \rightarrow Ag(NH_3)_2 + 2H_2O + Cl^- \qquad (a.1.2)$$
$$HNO_3 + NH_4OH \rightarrow NH_4NO_3 + H_2O \qquad (a.1.3)$$
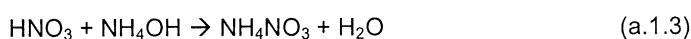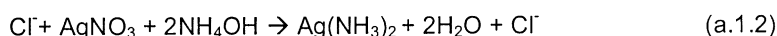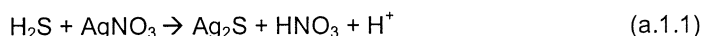
Similar to Backlund et al. (2005), immediately following the completion of a digestion, the reaction vessel was allowed to cool, the $AgNO_3$ trap was replaced with a fresh trap, and the reagent for the next digestion was added to the slurry already present in the reaction vessel via a syringe through the three-way valve. To prevent a build-up of pressure within the system, the cap for the $AgNO_3$ trap was always fitted loosely onto the centrifuge tube, with the assumption that the positive pressure created by the escaping excess gas is sufficient to prevent significant entrance of O_2 into the system through the end trap.

Carrying-out digestions under boiling conditions often resulted in bumping of the liquid in the reaction vessel, which increased in severity with each digestion as the volume of liquid in the reaction vessel is increased with the addition of each reagent to the slurry. This bumping is likely the result of the relatively tall and narrow design of the reaction vessels and has the potential to produce a back-pressure which can pull the contents of the $AgNO_3$ trap back through the system,

leading to low recovery of Ag_2S. For any instance in which contents of the $AgNO_3$ trap were pulled back through the system, the extraction was aborted, any Ag_2S precipitates were discarded, and fresh sample powder was submitted to digestion for another attempt of extracting the sulfur fractions. Teflon boiling beads added to the reaction vessel float in the reagent solutions and are thus ineffective in reducing bumping, however, chips of broken glass proved to be effective at decreasing the severity of bumping, and often prevented the drawback of the $AgNO_3$ trap solution. The glass chips used to decrease bumping were soaked in 10% HCl, rinsed three times with double-distilled water, dried at $100^{o}C$ overnight and cooled to room temperature prior to use with samples. In lieu of including a boiling bead equivalent to the reagent solution, use of a vessel that is much wider rather than tall and narrow as was used here may also prevent the occurrence of bumping of solutions within the reaction vessel.

AVS Recovery

Recovery of the AVS fraction was completed by following the general procedures presented by Tuttle et al. (1986). Via a syringe, 35mLs of a deaerated solution of 0.1M $SnCl_2$ in 6N HCl was introduced to the reaction vessel to produce H_2S from reaction of monosulfides with HCl (equation a.1.4). After 10 minutes at room temperature, the solution in the reaction vessel was boiled for five minutes then maintained at sub-boiling for 30 minutes. The heat was then turned off and after five minutes of cooling, the AVS digestion was considered complete and the $AgNO_3$ trap was replaced with a fresh trap.

$$FeS + 2HCl \rightarrow H_2S + FeCl_2 \qquad (a.1.4)$$

Experimental results indicate that stannous chloride ($SnCl_2$) in the reagent solution can lead to the reduction and recovery of up to 5% of the pyrite (equation a.1.5) present during the AVS digestion (Backlund et al., 2005; Chanton and Martens, 1985; Rice et al., 1993; Tuttle et al., 2003). However, due to the presence of iron oxides (Hematite = $Fe_2^{3+}O_3$, Magnetite = $Fe^{2+}O \cdot Fe^{3+}_2O_3$) and griegite ($Fe^{2+}Fe_2^{3+}S_4$) in some of the samples, it is necessary to include $SnCl_2$ in the reagent solution in order to prevent the oxidation of evolved H_2S to elemental sulfur (S^o) by ferric iron (Fe^{3+}) (equation a.1.6 & a.1.7) (Backlund et al., 2005; Pruden and Bloomfield 1986; Rice et al., 1993; Tuttle et al., 1986; Tuttle et al., 2003).

$$Sn^{2+}Cl_2 + 4HCl + Fe^{2+}S_2^- \rightarrow 2H_2S^{2-} + Fe^{2+} + Sn^{4+}Cl_4 \qquad (a.1.5)$$
$$H_2S^{2-} + 2Fe^{3+} \rightarrow S^o + 2H^+ + 2Fe^{2+} \qquad (a.1.6)$$
$$H_2S + 2Fe^{3+} + 3SnCl_2 \rightarrow H_2S + 2H^+ + 3Sn^{2+} + 2FeCl_3 \qquad (a.1.7)$$
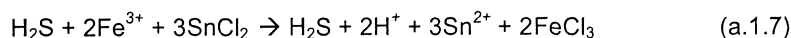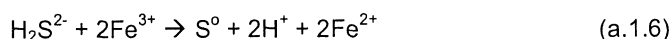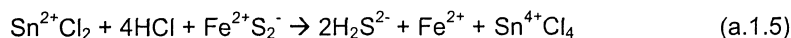
Prevention of H_2S oxidation is crucial because S^o is not extractable during AVS digestion, but is extractable by the CRS digestion, and hence the oxidation of H_2S produced during the AVS digestion results in a misrepresentation of sulfur present in both the AVS and the CRS fractions (Rice et al., 1993). Thus, to ensure maximum recovery of the pyrrhotite, pentlandite, chalcocite and greigite during the AVS extraction, $SnCl_2$ was included in the reagent solution. However, in light of possible consequential partial recovery of pyrite during the AVS digestion, the timing of the steps in the AVS reaction procedure were strictly adhered to for all samples and the reaction was terminated after 30 minutes of sub-boiling, regardless of if there appeared to still be active precipitation of Ag_2S in the $AgNO_3$ trap.

CRS Recovery

Following procedures presented by previous investigators (Canfield et al., 1986; Tuttle et al., 1986; Zhabina and Volkov, 1978) a solution of 1M chromous chloride ($CrCl_2$) in 0.5N HCl was used to reduce the sulfur of any remaining sulfides to S^{2-} via the oxidation of $CrCl_2$ (Newton et al., 1995) which then produces H_2S from reaction with the acidic solution (equation a.1.8). This reduced solution is easily oxidized by atmospheric air (Canfield et al., 1986), and thus a fresh solution was prepared in the laboratory prior to the commencement of sulfur extractions by passing a solution of 1M chromic chloride ($CrCl_3$) in 0.5N HCl through a Jone's reductor. Use of this apparatus results in the reduction of Cr^{3+} in the chromic chloride solution to Cr^{2+} via oxidation of a column of amalgamated zinc pellets (equation a.1.9) (Skoog et al., 1992) thereby producing a fresh acidic chromous chloride solution that was stored in a reagent bottle with a glass ground stopper until use.

$$4H^+ + 2Cr^{2+} + FeS_2^- \rightarrow 2H_2S^{2-} + 2Cr^{3+} + Fe^{2+} \qquad (a.1.8)$$

$$Zn(Hg) + 2Cr^{3+}Cl_3 \rightarrow Zn^{2+} + Hg^o + 2Cr^{2+}Cl_2 + 2Cl^- \qquad (a.1.9)$$
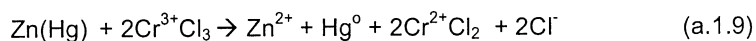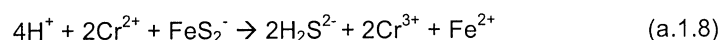
For CRS digestion, 35mLs of the reagent solution was added to the reaction vessel via a syringe immediately following the replacement of the $AgNO_3$ trap after the AVS extraction. The slurry in the reaction vessel was then boiled for approximately 1-2 hours. As it has been shown that this digestion procedure does not digest any sulfates (Canfield et al., 1986; Zhabina and Volkov, 1978), the reaction was continued until there was no more active precipitation of Ag_2S in the $AgNO_3$ trap. After Ag_2S precipitation ceased, the CRS digestion step was considered complete, and the vessel was allowed to cool for 10 minutes prior to the replacement of the $AgNO_3$ trap.

The chromous chloride reagent will digest any form of reduced inorganic sulfur present (Canfield et al., 1986) by either equation a.1.8 and or equation a.1.5, and thus the extraction of the CRS fraction using this solution was applied following AVS extraction in an attempt to collect

separate fractions of monosulfide- and disulfide-sulfur. Although applying the digestion procedures in this order allows for all recovered pyrrhotite, pentlandite, and chalcocite to be collected in the AVS fraction, we emphasize that neither bornite nor chalcopyrite is fully recoverable during the AVS digestion, and consequently significant portions of bornite (43%) and chalcopyrite (24%) are included in the CRS fraction (Tuttle et al., 2003). Thus, it cannot be assumed that the AVS and CRS fractions constitute sulfur from purely independent sulfide phases.

Sulfate Recovery

Following the replacement of the $AgNO_3$ trap after completion of the CRS extraction, 35mLs of a solution modified from that used by Thode et al. (1961) was introduced to the reaction vessel through the three-way valve via a syringe. Application of this reagent results in the reduction of both inorganic and organic forms of sulfate (SO_4^{2-}) to H_2S via the oxidation of hydriodic acid (HI) and hypophosophorous acid (H_2PO_3) (Norwitz, 1971; Pepkowitz and Shirley, 1951) while also causing a double displacement reaction between the sulfate compound and HCl in the reagent to form H_2O and a chloride compound (equation a.1.10). Thus, any sulfates present in the sample are reduced and any O_2 gas evolved as a byproduct of the reduction is retained in the slurry in the reaction vessel as H_2O. The reaction was carried out for two to three hours until there was no more active precipitation of Ag_2S in the $AgNO_3$ trap. After Ag_2S precipitation stopped, the reaction vessel was allowed to cool for 10 minutes, and the $AgNO_3$ trap was removed from the apparatus and capped.

$$H_3PO_2 + 2HI + CaSO_4 + 4HCl \rightarrow H_3PO_4 + I_2^{o} + H_2S + 2H_2O + CaCl_2 \qquad (a.1.10)$$
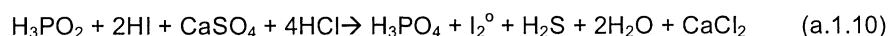
Hydriodic acid is easily oxidized by light and air (Brady and Holum, 1993), and thus the reagent solution used for the sulfate digestion is unstable over long periods of time. Hence, the reagent was prepared in the laboratory according to established procedures (Thode et al., 1961) within days prior to extractions. Pre-purified N_2 gas was bubbled through a boiling mixture of 65% HI (47% HI stabilized with 1.5% H_3PO_2), 25% hypophosphorous acid (50% H_3PO_2), and 10% concentrated HCl for 2 hours to ensure that the solution was free of any sulfur species. After cooling, the solution was then stored in a brown glass reagent bottle with a ground glass stopper until use. In application of this reagent, all sulfides, elemental sulfur, and sulfates will be digested (Pepkowitz and Shirley, 1951) and thus in order to extract separate sulfur fractions, this reagent was the last to be applied in the extraction procedure. Accordingly, due to HCl already present in the reaction vessel following the AVS and CRS digestions, the percentages of the separate acids used in preparation of the reagent solution as listed above are modified from those originally prescribed by Thode et al. (1961).

Cleaning

Between samples, the extraction apparatus was dismantled and all glassware, fittings and tubing was rinsed three times with deionized water, followed by 3 rinsings with double distilled water and dried at room temperature overnight. Following unsuccessful extractions that resulted in the drawback of Ag_2S through the system, all fittings and glassware parts were soaked in a ~1.23% bleach solution (Regular Chlorox Bleach diluted to 1 part Chlorox : 4 parts DD water) for a minimum of one hour between the deionized water and double distilled water rinsings, and tubing was replaced.

Sulfur Contents and Preparation for Isotopic Analysis

Ag_2S precipitates from each $AgNO_3$ trap were later filtered onto separate 0.45 μm silver filters (Spi supplies) and rinsed with double-distilled water. Silver filters were chosen because their robustness allows for easy handling relative to other standard membrane filters. Additionally, as a benefit of the pure Ag composition of the filters, physical transfer of the Ag_2S precipitate from the filter will not result in contamination of the sample by sulfur or other chemical components present in many of the common fiber and membrane filter types (Ali and Basco, 1996; Kowalenko and Grimmett, 2008). Following filtration, filters and Ag_2S were then placed onto open Petri dishes (Falcon, 50 x 9mm, sterile) and allowed to dry in a dessicator with silica gel overnight to remove excess moisture. Weight of recovered Ag_2S precipitates was determined gravimetrically by difference to 0.1 mg and was used to determine the weight of sulfur that was extracted for the respective sample fraction (equation a.1.11). If at least 1mg of Ag_2S precipitate for a single fraction was extracted, the Ag_2S was transferred to a clean vial for storage and was submitted for isotope analysis.

$$\text{S contents (ppm)} = \frac{W_{Ag2S}/W_{rock}}{MW_{Ag2S} \times MW_S} \times 10^6 \qquad \text{(a.1.11)}$$

Where:
W_{Ag2S} = weight of Ag_2S precipitate (g)
W_{rock} = weight of rock powder sample (g)
MW_{Ag2S} = molecular weight of Ag_2S = 247.8024 (g/mol)
MW_S = molecular weight of S = 32.066 (g/mol)

APPENDIX 2. Results of representative electron microprobe analyses from the Leg 176 section of Hole 735B.

Lith. Unit-Alt. Zone	Core-Section, interval (cm)	Description	Elements (Wt %)					
			S	Fe	Co	Ni	Cu	Total
1-VII	99R-1, 113-118	CT-2-SM-V	28.39	4.33	0.01	----	57.04	89.76
		PY-1-SM-I	52.55	44.02	0.36	1.37	0.16	98.46
1-XIII	103R-4, 72-76	CP-1-CC-V	35.05	29.69	0.09	0.02	33.79	98.63
		G-1-SM-I	41.16	55.96	0.16	0.46	0.03	97.76
		PO-2-SM-RO	39.86	59.30	0.12	0.06	0.03	99.37
2-IX	116R-3, 39-44	PY-2-CC-V	53.06	45.63	0.06	0.03	----	98.78
		PY-2-SM-V	53.16	46.20	0.07	0.01	----	99.43
		PY-2-FF-PL	53.06	45.87	0.06	----	0.01	99.01
		PY-2-FF-CPX	53.59	45.37	0.05	0.01	----	99.02
		PY-2-SM-RCPX	52.84	46.72	0.08	----	----	99.64
2-X	131R-1, 120-125	PY-2-SMT-ROL	52.29	46.23	0.17	0.13	0.01	98.84
		PY-2-SM-RO	52.07	46.13	0.09	0.07	----	98.36
		PY-2-FX-RO	51.95	46.18	0.08	0.08	----	98.29
		PO-2-FX-RO	38.78	59.93	0.09	0.01	----	98.82
		PO-1-SM-I	38.50	59.84	0.09	0.01	0.03	98.48
		PN-1-SM-I	33.41	32.45	7.05	25.87	0.12	98.90
		CP-1-SM-I	34.60	30.27	0.09	0.02	33.01	97.98
3-X	140R-1, 119-124	PY-2-Z-V	51.87	45.83	0.06	----	0.01	97.77
		PO-2-SM-RO	38.36	58.02	0.10	0.07	0.02	96.580
3-XI	159-2, 74-80	PY-2-FX-RO	52.24	45.91	0.08	0.05	----	98.27
		PO-2-SM-OPX	39.10	57.75	0.13	0.05	0.19	97.21
		PO-2-FX-RO	39.35	58.31	0.11	0.02	0.67	98.46
		PO-1-SM-I	39.60	59.19	0.10	0.14	0.03	99.05
		CP-1-SM-I	34.31	30.07	0.05	0.01	33.21	97.64
4-XI	177R-5, 61-66	CP-1-CC-I	37.06	29.45	0.04	0.10	33.74	100.38
		ID-1-CC-I	32.18	16.23	0.03	0.03	51.63	100.10
		XBN-1-CC-I	28.00	10.92	0.02	----	61.12	100.05
		PY-2-SM-V	56.32	46.36	0.08	----	----	102.76
		PN-1-SM-OL	35.01	28.41	2.11	35.41	0.16	101.11
		CP-1-SM-PL	37.10	29.97	0.04	----	33.86	100.97
		PO-1-SM-PL	40.94	59.30	0.10	0.04	0.68	101.05
		PN-1-SM-PL	35.09	33.74	2.82	29.59	0.06	101.29
		PO-2-SM-RO	38.17	59.03	2.19	0.20	----	99.59
5-XII	196R-5, 126-133	PO-2-SM-RO	38.28	61.83	0.10	0.01	----	100.22
		PO-2-CC-RO	38.32	61.77	0.10	----	----	100.19
		CP-2-SM-RO	35.98	30.20	0.04	0.01	33.65	99.88
		PN-2-SM-RO	35.38	21.67	11.86	31.66	0.04	100.60
		CP-1-Z-I	37.59	29.46	0.06	0.05	33.04	100.20
		PN-1-Z-I	34.96	24.26	4.280	36.56	0.08	100.14
		CP-2-Z-RPL	36.61	29.52	0.04	----	33.54	99.71

*Description: analyzed sulfide mineral-alteration type-associated alteration mineral-occurrence where PY = pyrite, PO = pyrrhotite, PN = pentlandite, CT = chalcocite, CP = chalcopyrite, ID = idaite, XBN = anomalous bornite, 1 = primary, 2 = secondary, CC = calcite, FX = iron-oxyhydroxide, SM = smectite, SMT = smectite-talc, Z = zeolite, FF = fracture filling, ROL = replacing olivine, RCPX = replacing clinopyroxene, RPL= replacing plagioclase, OL = in olivine, PL = in plagioclase, CP = in clinopyroxene, OPX = in orthopyroxene, V = vein, I = interstitial.

APPENDIX 3. Previously published sulfur contents and isotopic compositions from the Leg 118 section of Hole 735B.

Lithologic Unit	Alteration Zone	Section, interval (cm)	Depth (mbsf)	S Contents (ppm) Sulfide AVS	CRS	Sulfate	Total*	$\delta^{34}S$ (‰) Sulfide AVS	CRS	Sulfate	Total**
I	1'	2D-2, 140-144	10	30	40	---	100				
I		5D-1, 5-9	20	30	180	---	100		-1.1		
I		9D-1, 31-35	35	10	10	---	60				
II		13R-2, 75-79	45	140	140	10	290	0.2	0.2		0.9
II		17R-1 1-5	65	320	120	---	500		0.7		
II		24R-2, 132-136	105	20	30	---	140	6.9	0.8		3.2
II		30R-2, 82-87	140	120	130	30	320	2.6	-0.7	9.5	1.8
II		34R-2, 96-100	160	20	20	30	230		-10.8	21.8	
II		39R-2, 96-100	190	120	40	10	200	-2.8	-11.5		-3.3
III		43R-2, 86-90	210	370	300	---	780	-0.1	0.1		0.0
III		45R-2, 32-36	215	240	70	---	390	-1.0	-0.5	23.5	1.0
III		49R-2, 118-122	235	560	560	30	1090				
IV	2'	52R-2, 22-26	255	1150	1040	---	2010	-2.6	-2.1		-2.2
IV		53R-2, 53-57	260	1100	1130	20	2530	0.7	-0.1	3.2	0.5
IV		54R-4, 37-41	265	500	820	140	1210	0.0	-1.0		
V		58R-4, 54-58	285	280	240	250	730	-3.2	-16.6	21.0	0.5
V		62R-4, 89-93	305	190	100	---	290	2.6			
V		68R-2, 20-24	340	440	170	10	550	0.6	0.4		0.5
V		73R-2, 28-32	370	300	140	10	480	1.8			
VI		78R-2, 22-26	415	370	200	30	670	0.8	-0.5		1.4
VI		81R-2, 22-26	435	420	180	10	680	0.3			
VI		85R-2, 115-119	475	850	150	---	840	0.7	0.1		0.6

Lithologic Units as defined by Dick et al., (1991) and Alteration Zones as defined by Bach et al. (2001)
Sulfur data from (Alt and Anderson, 1991) where:
*Total Sulfur Content determined separately by a LECO CS-244 carbon-sulfur analyzer
**Where no $\delta^{34}S_{sulfate}$ was analyzed, Total $\delta^{34}S$ was calculated assuming $\delta^{34}S_{sulfate} = 21‰$
Blanks = not analyzed
--- = not detected

33

APPENDIX 4. Previously published sulfur contents from the Leg 176 section of Hole 735B

Sample ID	Section, interval (cm)	Depth (mbsf)	Total S Contents (ppm)
(F1)	91R-3, 125-130	521.23	300
(A1-2)	91R-3, 100-105	520.88	300
(A1-1)	91R-3, 90-95	520.98	200
(F2)	93R-1, 75-81	532.88	100
(A2)	93R-1, 86-91	532.99	200
(F3)	102R-3, 8-14	592.89	100
(A3)	102R-3, 1-8	592.83	100
(F4)	103R-2, 120-125	597.42	400
(A4)	103R-2, 139-142	597.6	100
(F5)	103R-4, 36-45	599.56	300
(A5)	103R-4, 18-22	599.35	300
(F6)	127R-5, 22-28	770.78	100
(A6)	127R-5, 12-20	770.69	200
(F7)	132R-1, 94-99	814.17	1800
(A7)	132R-1, 70-78	813.94	11800
(F8)	132R-8, 112-118	823.32	1000
(A8)	132R-8, 103-109	823.23	2400
(F9)	150R-3, 77-83	973.36	700
(A9)	150R-3, 65-69	973.23	600
(F10)	168R-3, 10-15	1133.02	600
(A10)	168R-3, 71-76	1133.63	800
(F11)	168R-7, 36-41	1139.05	700
(A11)	168R-7, 7-13	1138.75	400
(F12)	173R-4, 94-100	1183.61	800
(A12-1)	173R-4, 105-113	1183.73	4500
(A12-2)	173R-4, 115-119	1183.81	1700
(F13)	177R-5, 34-40	1207.41	400
(A13)	177R-5, 50-56	1207.57	2400
(F14)	180R-4, 93-100	1235.75	1300
(A14)	180R-4, 109-119	1235.92	1500
(F15)	188R-7, 61-68	1316	600
(A15)	188R-7, 101-107	1316.39	1500
(F16)	190R-2, 69-75	1327.95	600
(A16)	190R-2, 97-103	1328.23	2900
(F17)	207R-6, 32-38	1476.27	400
(A17)	207R-6, 32-38	1475.96	1500
(F18)	209R-4, 63-70	1493.67	600
(A18)	209R-4, 103-111	1493.67	500

Sulfur data as determined by a LECO sulfur determinator CS 225 by Bach et al. (2001) where:
"A" in sample ID indicates "altered"
"F" in sample ID indicates "fresh"

REFERENCES

Ali, A. E. and Bacso, J., 1996. Investigation of different types of filters for atmospheric trace elements analysis by three analytical techniques. *J. Radioanal. Nucl. Chem.-Artic.,* 209: 147-155.

Alt, J.C., 1995a. Subseafloor Processes in Mid-Ocean Ridge Hydrothermal Systems, In: S. Humphris, L. Mullineaux, R. Zierenberg and R. Thomson (Eds.): *Seafloor Hydrothermal Systems: Physical, Chemical, Biological, and Geological Interactions.* AGU Geophysical Monograph, 91: 85-114.

Alt, J.C., 1995b. Sulfur isotopic profile through the oceanic crust: Sulfur mobility and seawater-crustal sulfur exchange during hydrothermal alteration. *Geology,* 23: 585-588.

Alt, J.C., 2004. Alteration of the upper oceanic crust: mineralogy, chemistry, and processes. In: E.E. Davis and H. Elderfield (Eds.), *Hydrogeology of the Oceanic Lithosphere.* Cambridge University Press, New York, 497-595.

Alt, J.C., and Anderson, T.F., 1991. Mineralogy and isotopic composition of sulfur in layer 3 gabbros from the Indian Ocean, Hole 735B. In Von Herzen, R., Robinson, P.T., et al., Proc. ODP, Sci. Results, 118: College Station, TX (Ocean Drilling Program), 113–125. doi:10.2973/odp.proc.sr.118.155.1991

Alt, J.C. and Bach, W., 2006. Oxygen isotope composition of a section of lower oceanic crust, ODP Hole 735B, *Geochem. Geophy. Geosyst.,* 7. Q12008, doi:10.1029/2006GC001385

Alt, J.C. and Shanks, W.C., 1998. Sulfur in serpentinized oceanic peridoties: serpentinization processes and microbial sulfate reduction. *Journal of Geophysical Research,* 103: 9917-9929.

Alt, J.C., Davidson, G.J., Teagle, D.A.H, and Karson, J.A., 2003. Isotopic composition of gypsum in the Macquarie Island ophiolite: Implications for the sulfur cycle and the subsurface biosphere in oceanic crust. *Geology,* 31: 549-552

Anthony, J.W., Bideaux, R.A., Bladh, K.W., and Nichols, M.C., 1990. *Handbook of Mineralogy.* Mineral Data Publishing, Tucson, AZ.

Bach, W. and Edwards, K.J., 2003. Iron and sulfide oxidation within the basaltic ocdan crust: Implications for chemolithoautotrophic microbial biomass production. *Geochim. Cosmochim. Acta,* 67 (20): 3871-3887. doi:101.106/S0016-7037(00)00304-1

Bach, W., Alt, J.C., Niu, Y.L., Humphris, S.E., Erzinger, J., and Dick, H.J.B., 2001. The geochemical consequences of late-stage low-grade alteration of lower ocean crust at the SW Indian Ridge: Results from ODP Hole 735B (Leg 176). *Geochim. Cosmochim. Acta,* 65: 3267-3287.

Backlund, K., Boman, A., Frojdo, S. and Astrom, M., 2005. An analytical procedure for determination of sulphur species and isotopes in boreal acid sulphate soils and sediments. *Agr. Food Sci.,* 14: 70-82.

Beaudoin, G., Taylor, B.E., Rumble, D. and Thiemens, M., 1994. Variations in the sulfur isotope composition of troilite fro the Canon-Diablo iron meteorite. *Geochim. Cosmochim. Acta,* 58: 4253-4255.

Belzile, N., Chen, Y.w., Cai, M.F. and Li, Y.R., 2004. A review on pyrrhotite oxidation. *J. Geochem. Explor.,* 84: 65-76.

Brady, J.E. and Holum, J.R., 1993. *Chemistry: The Study of Matter and Its Changes.* John Wiley & Sons, Inc., New York.

Canfield, D.E., 2001. Biogeochemistry of sulfur isotopes. In: J.W. Valley and D.R. Cole (Eds.) *Reviews in Mineralogy and Geochemistry*. The Mineralogical Society of America, Blacksburg 43: 607-636.

Canfield, D.E., Raiswell, R., Westrich, J.T., Reaves, C.M. and Berner, R.A., 1986. The use of chromium reduction in the analysis of reduced inorganic sulfur in sediments and shales. *Chem. Geol.*, 54: 149-155.

Canfield, D.E. and Teske, A., 1996. Late Proterozoic rise in atmospheric oxygen concentration inferred from phylogenetic and sulphur-isotope studies. *Nature*, 54: 127-132.

Carbotte, S.M. and Scheirer, D.S., 2004. Variability of ocean crustal structure created along the global mid-ocean ridge. In: Davis, E.E. and Elderfield, H. (Eds.) *Hydrogeology of the Oceanic Lithosphere*. Cambridge University Press, New York, 59-106.

Chanton, J.P. and Martens, C.S., 1985. The effects of heat and stannous chloride addition on the active distillation of acid volatile sulfide from pyrite-rich marine sediment samples. *Biogeochemistry*, 1: 375-383.

Coplen, T.B. and Krouse, H.R., 1998. Sulphur isotope data consistency improved. *Nature*, 392: 32.

Cowen, J.P., Giovannoni, S.J., Kenig, F., Johnson, H.P., Butterfield, D., Rappe, M.S., Hutnak, J. and Lam, P., 2003. Fluids from aging ocean crust that support microbial life. *Science*, 299: 120-123.

Craig, J.R. and Vaughan, D.J., 1981. *Ore Microscopy and Ore Petrography.* John Wiley & Sons, New York.

Davis, A.S., Clague, D.A., Zierenberg, R.A., Wheat, C.G. and Cousens B.L., 2003. Sulfide formation related to changes in the hydrothermal system on Loihi Seamount, Hawai'I, following the seismic event in 1996. *Can. Mineral.*, 41: 457-472.

Dick, H.J.B., Meyer, P.S., Bloomer, S., Kirby, S., Stakes, D., and Mawer, C., 1991. Lithostratigraphic evolution of an in-situ section of oceanic layer 3. In Von Herzen, R., Robinson, P.T., et al., Proc. ODP, Sci. Results, 118: College Station, TX (Ocean Drilling Program), 439–538. doi:10.2973/odp.proc.sr.118.128.1991

Dick, H.J.B., Natland, J.H., Alt, J.C., Bach, W., Bideau, D., Gee, J.S., Haggas, S., Hertogen, J.G.H., Hirth, G., Holm, P.M., Ildefonse, B., Iturrino., G.J., John, B.E., Kelley, D.S., Kikawa, E., Robinson, P.t., Snow, J., Stephen , R.A., Trimby, P.W., Worm, H.U. and Yoshinobu, A., 2000. A long in-situ section of the lower ocean crust: results of ODP Leg 176 drilling at the Southwest Indian Ridge. *Earth Planet. Sci. Lett.*, 179: 31-51

Edmond, J.M., Measures, C., McDuff, R.E., Chan, L.H., Collier, R., Grant, B., Gordon, L.I. and Corliss, J.B., 1979a. Ridge crest hydrothermal activity and the balances for the major and minor elements in the ocean – Galapagos data. *Earth Planet. Sci. Lett.*, 46: 1-18.

Edmond, J.M., Measures, C., Measures, C., Mangum, B., Grant, B., Sclater, F.R., Collier, R., Hudson, A., Gordon., L.I. and Corliss, J.B., 1979b. Formation of metal-rich deposits at ridge crests. *Earth Planet. Sci. Lett.*, 46: 19-30.

Edwards, K.J., Bach, W. and McCollom, T.M., 2005. Geomicrobiology in oceanography: microbe-mineral interactions at and below the seafloor. *Trends Microbiol.*, 13: 449-456. doi:10.1016/j.tim.2005.07.005

Fisher, A.T., 1998. Permeability within basaltic oceanic crust, *Rev. Geophys.*, 36: 143-182.

Fisk, M.R., Giovannoni, S.J., and Thorseth, I.H., 1998. Alteration of oceanic volcanic glass: Textural evidence of microbial acitivity. *Science*, 281: 978-980.

Furnes, H. and Staudigel, H., 1999. Biological mediation in ocean crust alteration: how deep is the deep biosphere? *Earth Planet. Sci. Lett.*, 166: 97-103.

Goldstein, T.P. and Aizenshtat, Z., 1994. Thermochemical sulfate reduction – A review. *J. Therm. Anal.*, 42: 241-290.

Huber, J.A., Johnson, H.P. Butterfield, D.A. and Baross, J.A., 2006. Microbial life in ridge flank crustal fluids. *Eviron. Microbiol.*, 8: 88-99.

Hutnak, M., Fisher, A.T., Harris, R., Stein, C., Wang, K., Spinelli, G., Schindler, M., Villinger, H. and Silver, E., 2008. Large heat and fluid fluxes driven through mid-plate outcrops on ocean crust. *Nat. Geosci.*, 1: 611-614. doi:10.1038/ngeo264

Jacobson, R.S., 1992. Impact of crustal evolution on changes of the seismic properties of the uppermost ocean crust. *Rev. Geophys.*, 30: 23-42.

Jørgensen, B.B., Isaksen, M.F. and Jannasch, H.W., 1992. Bacterial sulfate reduction above 100-degrees-C in deep-sea hydrothermal vent sediments. *Science*, 258: 1756-1757.

Kaplan, I.R. and Rittenberg, S.C., 1964. Microbiological fractionation of sulphur isotopes. *Microbiology*, 34: 195-212.

Karson, J.A., 1998. Geological investigation of a lineated massif at the Kane Transform Fault: implications for oceanic core complexes. *Phil. Trans.: Mathematical, Physical and Engineering Sci.*, 357 (1753): 713-740.

Knipe, S.W., Mycroft, J.R., Pratt, A.R., Nesbitt, H.W. and Bancroft, G.M., 1995. X-ray photoelectron spectroscopic study of water-adsorption on iron sulfide minerals. *Geochim. Cosmochim. Acta*, 59: 1079-1090.

Kowalenko, C.G. and Grimmett, M., 2008. Chemical characterization of soil sulfur. In: M.R. Carter and E.G. Gregorich (Eds.), *Soil Sampling and Methods of Analysis*. CRC Press, Boca Raton, FL. 251-263.

Lister, C.R.B., 1982. "Active" and "passive" hydrothermal systems in the ocean crust. Predicted physical condition. In: K.A. Fanning and F.T. Manheim (Eds.), *The Dynamic Environment of the Ocean Floor*. D.C. Heath, Lexington, MA. 441-470.

Madigan, M.T. and Martinko, J.M., 2006. *Brock Biology of Microorganisms*. Pearson Prentice Hall, Upper Saddle River, NJ.

Malinin, S.D. and Khitarov, N.I., 1969. Reduction of sulfate sulfur by hydrogen under hydrothermal conditions. *Geochemistry International Ussr*, 6: 1022-1027.

McKinley, J.P., Stevens, T.O. and Westall, F., 2000. Microfossils and paleoenvironments in deep subsurface basalt samples. *Geomicrobiol. J.*, 17: 43-54.

Miller, D.J., and Cervantes, P., 2002. Sulfide mineral chemistry and petrography and platinum group element composition in gabbroic rocks from the Southwest Indian Ridge. In Natland, J.H., Dick, H.J.B., Miller, D.J., and Von Herzen, R.P. (Eds.), Proc. ODP, Sci. Results, 176, 1–29. doi:10.2973/odp.proc.sr.176.009.2002

Natland, J.H., Dick, H.J.B., Miller, D.J., and Von Herzen, R.P. (Eds.), 2002. Proc. ODP, Sci. Results, 176: College Station, TX (Ocean Drilling Program). doi:10.2973/odp.proc.sr.176.2002

Newton, R.J., Bottrell, S.H., Dean, S.P., Hatfield, D., and Raiswell, R., 1995. An evaluation of the use of the chromous chloride reduction method for isotopic analyses of pyrite in rocks and sediment. *Chem. Geol.*, 125: 317-320.

Norwitz, G., 1971. Spectrophotometric determination of sulphate in propellants and nitrocellulose. *Analyst*, 96: 494-501.

Ohmoto, H. and Goldhaber, M.B., 1997. Suflur and Carbon Isotopes. In: Hubert, L.B. (Ed.), *Geochemistry of Hydrothermal Deposits.* Wiley & Sons, New York. 517-612.

Ohmoto, H. and Lasaga, A.C., 1982. Kinetics of reactions between aqueous sulfates and sulfides in hydrothermal systems. *Geochim. Cosmochim. Acta*, 46: 1727-1745.

Ohmoto, H. and Rye, R.O., 1979. Isotopes of sulfur and carbon. In: Barnes, H.L. (Ed.), *Geochmistry of Hydrothermal Ore Deposits.* Wiley & Sons, New York. 509-567.

Pepkowitz, L.P. and Shirley, E.L., 1951. Microdetection of sulfur. *Anal. Chem.*, 23: 1709-1710.

Pilson, M.Q., 1988. *An Introduction to the Chemistry of the Sea.* Prentice Hall, Upper Saddle River.

Pruden, G. and Bloomfield, C., 1968. The determination of iron(II) sulphide in soil in the presence of iron(III) oxide. *Analyst*, 93: 532-534.

Rice, C.a., Tuttle, M.L. and Reynolds, R.L., 1993. The analysis of forms of sulfur in ancient sediments and sedimentary rocks – Comments and cautions. *Chem. Geol.*, 107: 83-95.

Robb, L.J., 2004. *Introduction to ore-forming processes.* Blackwell Pub., Malden, MA.

Rouxel, O., Ono, S.H., Alt, J., Rumble, D. and Ludden, J., 2008. Sulfur isotope evidence for microbial sulfate reduction in altered oceanic basalts at ODP Site 801. *Earth Planet. Sci. Lett.*, 268: 11-123. doi:10.1016/j.epsl.2008.01.010.

Sakai, H., Desmarais, D.J., Ueda, A. and Moore, J.G., 1984. Concentrations and isotope ratios of carbon, nitrogen and sulfur in ocean-floor basalts. *Geochim. Cosmochim. Acta*, 48: 2433-2441.

Schoonen, M.A.A. and Barnes, H.L., 1991. Reactions forming pyrite and marcasite from solutions. 2. Via FeS precursors below 100-degrees-C. *Geochim. Cosmochim. Acta*, 55: 1505-1514.

Schulz, H.N. and Jørgensen, B.B., 2001. Big bacteria. *Annu. Rev. Microbiol.*, 55: 105-137.

Seal, R.R.I., 2006. Sulfur isotope geochemistry of sulfide minerals. *Reviews in Mineralogy and Geochemistry.* The Mineralogical Society of America, Blacksburg 61: 633-677.

Shan, X.Q. and Chen, B., 1995. Determination of carbon-bonded sulfur in soils by hydriodic acid reduction and hydrogen-peroxide oxidation. *Fresenius J. Anal. Chem.*, 351: 762-767.

Shipboard Scientific Party, 1999. Leg 176 summary. In Dick, H.J.B., Natland, J.H., Miller, D.J., et al., Proc. ODP, Init. Repts., 176: College Station, TX (Ocean Drilling Program), 1–70. doi:10.2973/odp.proc.ir.176.101.1999

Skoog, D.A., West, D.M. and Holler, F.J., 1992. *Fundamentals of analytical chemistry.* Saunders College Pub., Fort Worth, TX. 371-372.

Small, J.S., Hamilton, D.L. and Habesch, S., 1992. Experimental simulation of clay precipitation within reservoir sandstones .1. Techniques and examples. *Journal of Sedimentary Petrology*, 62; 508-519.

Snoeyink, V.L. and Jenkins, D., 1980. pC-pe diagram for nitrogen system. In: *Water Chemistry.* John Wiley & Sons, Inc., New York. 406.

Stevens, T.O. and McKinley, J.P., 2000. Abiotic controls on H_2 production from basalt-water reactions and implications for aquifer biogeochemistry. *Environ. Sci. Technol.*, 34: 826-831.

Thode, H.G., Monster, J. and Dunford, H.B., 1961. Sulfur isotope geochemistry. *Geochim. Cosmochim. Acta*, 25: 159-174.

Thomas-Keprta, K.L., McKay, D.S., Wentworth, S.J., Stevens, T.O., Taunton, A.E., Allen, C.C., Coleman, A., Gibson, E.K. and Romanek, C.S., 1998. Bacterial mineralization patterns in basaltic aquifers: Implications for possible life in martian meteorite ALH84001. *Geology*, 26: 1031-1034.

Torsvik, T., Furnes, H., Muehlenbachs, K., Thorseth, I.H. and Tumyr, O., 1998., Evidence for microbial activity at the glass-alteration interface in oceanic basalts. *Earth Planet. Sci. Lett.*, 162: 165-176.

Tuttle, M.L., Goldhaber, M.B. and Williamson, D.L., 1986. An analytical scheme for determining forms of sulfur in oil shales and associated rocks. *Talanta*, 33: 953-961.

Tuttle, M.L.W., Briggs, P.H. and Berry, C.J., 2003. A method to separate phases of sulphur in mine-waste piles and natural alteration zones, and to use sulphur isotopic compositions to investigate release of metals and acidity to the environment. *Sixth International Conference on Acid Rock Draininage,* Caines, Australia.

Velbel, M.A. and Barker, W.W., 2008. Pyroxene weathering to smectite: conventional and cryo-field emission scanning electron microscopy, Koua Bocca ultramafic complex, Ivory Coast. *Clay Clay Min.*, 56: 112-127. doi: 10.1346/CCMN.2008.0560110.

Wirsen, C.O., Brinkhoff, T., Kuever, J., Muyzer, G., Molyneaux, S. and Jannasch, H.W., 1998. Comparison of a new *Thiomicrospira* strain from the Mid-Atlantic Ridge with known hydrothermal vent isolates. *Applied and Environmental Microbiology*, 64: 4057-4059.

Wirsen, Co., Jannashc, H.W. and Molyneaux, S.J., 1993. Chemosynthetic microbial activity at Mid-Atlantic Ridge hydrothermal vent sites. *J. Geophys. Res.-Solid Earth*, 98: 9693-9703.

Zhabina, N.N. and Volkov, I.I., 1978. A method of determination of various sulfur compounds in sea sediments and rocks. In: Krumbein, W.E. (Ed.), *Enviornmental Biogeochemistry and Geomicrobiology.* Ann Arbor Science, Ann Arbor MI. 735-746.

Zindler, A. and Hart, S., 1986. Chemical Geodynamics. *Annu. Rev. Earth Planet. Sci.*, 14: 493-571.